Accepted Manuscript

Specific features of HIV-1 integrase inhibition by bisphosphonate derivatives

Julia Agapkina, Dmitry Yanvarev, Andrey Anisenko, Sergey Korolev, Jouko Vepsäläinen, Sergey Kochetkov, Marina Gottikh

PII: S0223-5234(13)00770-8

DOI: 10.1016/j.ejmech.2013.11.028

Reference: EJMECH 6574

To appear in: *European Journal of Medicinal Chemistry*

Received Date: 16 September 2013

Revised Date: 24 November 2013

Accepted Date: 27 November 2013

Please cite this article as: J. Agapkina, D. Yanvarev, A. Anisenko, S. Korolev, J. Vepsäläinen, S. Kochetkov, M. Gottikh, Specific features of HIV-1 integrase inhibition by bisphosphonate derivatives, *European Journal of Medicinal Chemistry* (2014), doi: 10.1016/j.ejmech.2013.11.028.

Inhibition of the catalytic activity of HIV-1 integrase

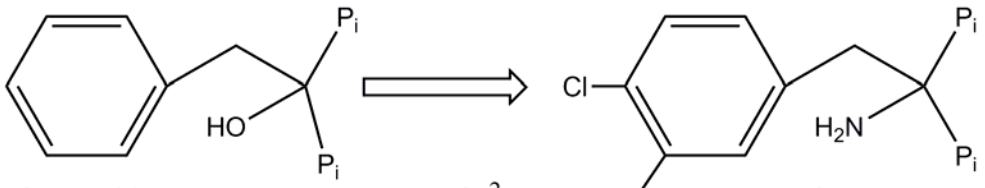

$IC_{50} > 500\ \mu M$ $P_i = PO_3^{2-}$ $IC_{50} = 7\ \mu M$

17 bisphosphonates of 5 different groups were synthesized including 3 earlier unknown

6 compounds inhibited both strand transfer and 3'-processing catalyzed by integrase

SAR study has been reported and explained using liquid NMR experiments

OH / NH_2 in the chelating group switches competitive inhibitor into noncompetitive

Specific features of HIV-1 integrase inhibition by bisphosphonate derivatives

Julia Agapkina[a,‖], Dmitry Yanvarev[*,b,‖], Andrey Anisenko[a], Sergey Korolev[a], Jouko Vepsäläinen[c], Sergey Kochetkov[b, a], Marina Gottikh[a]

[a]*-Lomonosov Moscow State University, Chemistry Department and Belozersky Institute of Physical and Chemical Biology, Moscow, Russia;* [b]*-Engelhardt Institute of Molecular Biology, Russian Academy of Sciences, Moscow, Russia;* [c] *-School of Pharmacy, Biocenter Kuopio, University of Eastern Finland, Kuopio, Finland.*

‖ these authors contributed equally to this work

***corresponding author**: Dmitry V. Yanvarev. E-mail: JDmitry@hotmail.com, tel.+79267025449

Abstract

The integration of viral DNA into the cell genome is one of the key steps in the replication cycle of human immunodeficiency virus type 1 (HIV-1). Therefore, the viral enzyme integrase (IN) catalyzing this process is of great interest as a target for new antiviral agents. We performed a structural-functional analysis of five different series of methylene bisphosphonates (BPs), PO_3H_2-C(R)(X)-PO_3H_2, as IN inhibitors with the goal of assessing structural elements required for the inhibitory activity. We found that IN is inhibited only by BP bearing a chlorobenzyl substituent R at the bridging carbon of the P-C-P backbone. These BP inhibited both IN-catalyzed reactions with similar efficacies. They were also active toward some INs with mutations characteristic for HIV-1 strains resistant to strand transfer inhibitors. The study of the mechanism of the IN inhibition by various BP showed that it is effected by the nature of the second substituent (X) at the bridging carbon. Among the tested compounds, only the BP with the amino group bound directly to the BP bridging carbon was found to be a noncompetitive inhibitor and, hence, it can be promising for further studies as potential inhibitor of the IN activity within the preintegration complex.

Keywords

HIV, integrase, bisphosphonates, inhibitors, SAR

1. Introduction

One of the key steps of the HIV-1 life cycle is the integration of the viral DNA copy into the host genome. This process is catalyzed by a viral enzyme called integrase (IN). When the reverse transcription of the viral genome is completed, IN binds to its DNA copy and catalyzes the 3'-processing resulting in the cleavage of GT nucleotides from both DNA 3'-ends. Then IN catalyzes the strand transfer reaction, that is, the integration of the viral DNA to the host cell

DNA, to form a provirus. Further regulated expression of the proviral genome and assembling give new virions, which leave the cell and infect other cells.

Figure 1.

Integrase is of great interest as a target for the search of new antiviral agents, since, unlike other viral enzymes, it has no cell analogues and its inhibitors must not affect normal cell processes [1],[2]. Several types of integration inhibitors differing in the mechanism of action have been reported, but only two compounds, raltegravir and elvitegravir, are currently used for the treatment of HIV-infection as components of highly active antiretroviral therapy (HAART) [3],[4]. Both of them inhibit the IN function at the strand transfer stage by a similar mechanism, which results in the emergence of viral cross-resistance to these drugs [5],[6],[7]. Dolutegravir, a strand transfer inhibitor (INSTI) of the second generation, which is currently under phase III of clinical trials, is active toward some raltegravir-resistant HIV-1 strains. However, the partial cross-resistance with raltegravir and elvitegravir has been already found for this compound [7],[8]. Taking into consideration the above facts the optimal way for designing new integration inhibitors seems to be the search for the compounds with the mechanism of action differing from that of raltegravir and its analogues. Such inhibitors may be active toward INSTI resistant viral strains.

Phosphonates being hydrolytically stabile analogs of biogenic phosphates are widely used in antiviral drug design [9], [10], [11], [12].

Methylenebisphosphonates (BPs) are mimics of inorganic pyrophosphate, a substrate of HIV-1 reverse transcriptase (RT) in the pyrophosphorolysis reaction. These compounds can inhibit the cleavage of monophosphates of RT nucleoside inhibitors, which is the key reason for the HIV-1 resistance to azidothymidine and its analogues [13],[14]. Previously we found that some BPs can also inhibit HIV-1 IN at micromolar concentrations [15]. This allowed us to regard them as inhibitors of the new generation capable of inhibiting two viral enzymes operating at the early stage of viral infection.

In this work we studied the BP structure-activity relationship toward IN inhibition with the goal of evaluating their mechanism of action and optimizing their structure. Only BPs bearing a chlorobenzyl residue as a substituent R (Fig. 1) were found to display inhibitory properties. They inhibited both IN-catalyzed reactions with similar efficacies. These BPs were also active toward some INs with mutations inherent for drug-resistant HIV-1 strains. For the evaluation of the inhibition mechanism, kinetic models were designed, which demonstrated that the nature of the substituent X as well as the metal-cofactors, Mg^{2+} and Mn^{2+}, affected this

mechanism. This conclusion was also supported by the results of studies of the BP effect on the IN-DNA binding and IN catalytic activity within the IN-LEDGF complex.

2. Results

2.1 Chemistry

Seventeen bisphosphonates of five different groups were synthesized including earlier unknown (**3b**), (**3e**)**,** and (**4c**) (Fig. 1). The compounds (**1a**) [16], (**1b**) [17], (**1d**) [18], (**2a**) [14], (**2c**) [19], (**3a**) [20], (**3c**) [21], (**3d**) [19], (**5**) [19], (**6**) [22] were synthesized as earlier described with minor modifications. General synthetic procedures and physicochemical characteristics of all the prepared BPs are presented in Materials & Methods and SI.

Four general methods used are known from literature [17],[23],[24]. In brief, involved either (**A**)- phosphonylation of a carboxylic acid that resulted (**1a**, **1b**, **1c**, **3a**, **3c-e**) or a corresponding nitrile that afforded (**1d**, **2c, 3b**). (**B**)- Michael addition of amine to vinylidenediphosphonic acid to prepare (**4a-c**). (**C**)- Reaction of a acylphosphonate with dialkylphosphite followed by removal of alkoxy group with TMSBr (**2a**, **2b**). (**D**)- Reaction of benzylchlorides with sodium salt of methylenediphosphonic acid tetraester yielded (**2d**, **5**).

Vinylidenediphosphonic acid (VDPA) for synthesis of BPs **4a-c** was prepared using the optimization of the procedures described in the patent [25]. We used different thermal conditions for pyrolysis of etidronate to reach its 100% conversion and we modified procedure for VDPA deionization to avoid using strong ion-exchange resins and H_2SO_4 which yields to partial hydration of VDPA.

2.2. SAR analysis of the BP anti-integrase activity

Recently we demonstrated the capacity of two BPs bearing aromatic substituents to inhibit the IN-catalyzed 3'-processing [15]. Here we report the results of a structural analysis of a series of BPs in the attempt to find structural peculiarities essential for the inhibition of HIV-1 IN.

First, we analyzed the dependence of the BP inhibitory activity in 3'-processing reaction versus the substituent R structure (Fig. 1) and found that only compounds with a chlorobenzyl radical as the substituent R were active (Fig. 1, compounds **2a-d**, and **5**). Their inhibitory activities are presented in Table 1 (column 3); all other compounds were not active up to 250 μM concentration. We assumed that the reason for this effect could be the electron deficiency of the aromatic ring due to electron acceptor properties of the chlorine atom. To confirm this hypothesis, we synthesized compounds **3a-e** containing cationic pyridinium residues, which are more electron deficient than chlorobenzyl groups. However, these compounds did not inhibit IN

up to concentrations of 250 μM. It is also noteworthy that compound **2b**, although lacking the chlorine atom at the *meta*-position and, hence, less electron deficient, was a more effective inhibitor than the corresponding 3,4-dichlorobenzyl derivative **2a** (Table 1, column 3). These results imply that a chlorine atom at the *para*-position of the aromatic ring is necessary for BPs to display inhibitory properties. Compound **5** bearing two 3,4-dichlorobenzyl residues was somewhat a more effective inhibitor than compounds **2a**, **2c,** and **2d** containing one 3,4-dichlorobenzyl residue, but its activity was comparable with that of the monochlorobenzyl derivative **2b**. It should be noted that a halogen-containing aromatic residue is a mandatory structural element of all efficient INSTIs [1],[2],[8],[26] and some of 3'-processing inhibitors [27],[28],[29]. In the case of INSTIs, a halogenated benzyl group was shown to be involved in stacking interactions with the cytosine of the conserved CA dinucleotide forcing the 3′-OH of the terminal adenosine away from the IN active site [30],[31]. However, the actual role of the halogen atom in this process has been vague so far.

It is known that BPs exhibit strong affinity to metal ions, in particular, Ca^{2+} and Mg^{2+} [32],[33]. We supposed that the BP inhibitory activity toward IN can be explained by their capacity to coordinate Mg^{2+} ions, which are bound by amino acids D64, D116, and E152 in the enzyme active site. The nature of the substituent X is likely to have a substantial impact on BP metal binding properties and, therefore, their inhibitory activity. Due to the oxygen lone electron pairs, the hydroxyl group at the P-C-P backbone (compound **2a**) can be involved in the coordination of the metal ion. However, the replacement of the hydroxyl group by the hydrogen atom (compound **2d**) did not change the inhibitory activity (Table 1, column 3). This result has thrown into doubt the assumption on the obligatory presence of the Mg^{2+}-coordinating site in the inhibitor structure. Therefore, we evaluated two dichlorobenzyl derivatives containing carboxyl and phosphonate fragments in place of the bisphosphonate backbone (compounds **6** and **7**). Both of them lacked the inhibitory activity up to the concentration of 500 μM. This result allowed us a conclusion that the bisphosphonate backbone is an obligatory structural element of the inhibitors of this type.

The most potent IN inhibition was observed for compound **2c**, which had an amino group at the P-C-P backbone (Table 1, column 3). The transfer of the amino group into the linker that joins the P-C-P backbone and the aromatic fragment (compounds **4a**-**4c**) caused the complete loss of the BP inhibitory activity without regard to the position of the amino group in the linker or the presence of a halogen atom (iodine) in the aromatic ring.

Thus, the results of the SAR analysis showed that the BP inhibitory activity is determined by the presence of two structural moieties: a methylenediphosphonic backbone and a *p*-chlorobenzyl substituent.

2.3. The effect of the IN metal cofactor on the BP inhibitory activity

The absolute necessity of the P-C-P backbone for the BP inhibitory activity indicated that the latter may be associated with the coordination of the metal ion. With the goal of testing this assumption we studied the inhibition of 3'-processing and strand transfer reactions in the presence of two IN metal cofactors, Mg^{2+} and Mn^{2+}, using the most active inhibitors **2a**, **2b**, **2c**, **2d**, and **5**.

First, we found that all the compounds inhibited the IN activity in both reactions. In the presence of Mg^{2+} ions, the efficiency of the 3'-processing and strand transfer inhibition was nearly the same for compounds **2d** and **5**; compound **2c** inhibited the strand transfer twice as effectively; and compounds **2a** and **2b** bearing a hydroxyl group in the P-C-P backbone somewhat better inhibited the 3'-processing (Table 1, columns 3 and 5).

In the presence of Mn^{2+} ions all the compounds inhibited both reactions with nearly the same efficiency (Table 1, columns 4 and 6). It is noteworthy that the inhibitory activities of compounds **2a**, **2b, 2d,** and **5** considerably grew under these conditions. It was especially noticeable for inhibitor **5** containing two 3,4-dichlorobenzyl residues. Also, the inhibitory activities of compounds **2a**, **2b,** and **2d** were comparable with that of compound **2c**, whereas they markedly differed in the presence of Mg^{2+}.

In accordance with these results, all the tested BPs could be divided into two groups: group I, which included only compound **2c** with an amino group at the P-C-P backbone, and group II, with all the rest BPs (compounds **2a**, **2b, 2d,** and **5**). The fact that the metal nature was essential for the inhibitory activity of only group II inhibitors allowed us to make two assumptions. First, the mechanism of the IN inhibition by compound **2c** was independent of the metal cofactor nature. Second, in the presence of different metal cofactors compounds of group II inhibited IN by different mechanisms. Thus, the inhibition mechanism was the same for both groups in the presence of Mn^{2+} and differed in the presence of Mg^{2+}.

2.4. NMR-studies of BP interactions with metal ions

The major reason for such a great difference in the behavior of the inhibitors of the two groups may be differences in electron structures of these compounds. One of these differences is the capacity of the amino group of compound **2c** (group I) to be protonated, whereas the substituents X in the group II compounds lack this property under the tested conditions. Evidently, a positive charge in the BP metal-binding site should affect its interaction with metal ions and, hence, the character of IN inhibition.

With the goal of evaluating the impact of X substituents on the BP binding to metal ions, we studied the distribution of the electron density in inhibitors **2a** and **2c** using NMR spectroscopy, which is an accurate and sensitive method characterizing the molecule structure in solution.

It was observed in ^{1}H NMR spectra that the electron density in the hydrocarbon backbones of these inhibitors was distributed in a different way. This can be explained by the electron withdrawing effect of the $^{+}NH_3$-function in compound **2c**. As is seen in Fig. S1 (see SI), compound **2c** is characterized by a decreased shielding and a downfield shift of proton resonances. For the linker -CH_2- group the reduction of the electron density resulted in a decrease in the bond lengths, and for the aromatic system, in a decrease in the electron density of the π-system. The synchronous downfield shift of the aromatic protons implies that the cationic function does not cause the redistribution of the π-system electron density. Nevertheless, $^{+}NH_3$-function can influence cation-π and anion-π interactions (reviewed in [34], which may be formed between the inhibitor and IN.

The effect of the X substituent on the interaction of compounds **2a** and **2c** with magnesium ions was studied using ^{31}P NMR spectroscopy. Unlike H- and HO-BPs, the shift of the phosphorus resonance of NH_2-BPs at pH close to pK_a of their amino group is much more pronounced [35]. This considerable downfield shift of the phosphorus resonance can be ascribed to deprotonation of the $^{+}NH_3$-group. This effect was detected for inhibitor **2c** (pK_a of its amino group is 8.3), whereas the resonance of compounds **2a** was nearly constant (Fig. 2A).

We also studied the interaction of compounds **2a** and **2c** with Mg^{2+} ions at pH 1, 7, and 9.5, i.e., for the amino group of the latter was completely protonated, partially protonated, and completely deprotonated, using the ^{31}P NMR line broadening method. This approach is based on the principle that formation of coordination bonds between Mg^{2+} and a phosphonate group causes the broadening of the phosphorus resonance in ^{31}P NMR [36] . As is seen in Fig. 2B, the broadening of the phosphorus resonance of the amino derivative **2c** at pH 7 and 9.5 occurs much more intensely than that of the hydroxyl analogue **2a**. Since this effect is based on the formation of coordination bonds between BP and Mg^{2+}, we believe that the P-C-P backbone of compound **2a** does not form coordination bonds with Mg^{2+}, whereas in the case of compound **2c** such bonds are formed. Moreover, the greater is the portion of nonprotonated NH_2-groups, the greater is the efficacy of their formation. These experiments evidenced that the lone electron pair of the nitrogen atom nonprotonated amino group of compound **2c** was involved in the formation of coordination bonds with Mg^{2+} ions.

It is noteworthy that the IN inhibition was studied at pH 7.2, that is, when the amino group of compound **2c** is nearly fully protonated (Fig. 2A) and thus not capable to coordinate

Mg^{2+} ions. However, the $^{+}NH_3$-group can also strengthen metal binding properties of compound **2c**. It is known that α-amino BPs have decreased pK_a of phosphonate groups if compared with the analogues bearing protons or hydroxyl groups at the P-C-P backbone (1–2 log units [33]). Such a decrease is a result of the considerable electron acceptor effect of the NH_3^{+}cation, which markedly enhances the coordination capacity of α-amino BPs toward bivalent metal ions.

When summarizing the above facts one can conclude that BP bearing amino groups in the P-C-P backbone possess some physicochemical and, probably, structural specific features, particularly, an increased acidity of protons of aromatic substituents and the capacity to coordinate Mg^{2+} ions. It is likely that these specific features lead to different mechanisms of IN inhibition by group I and II BPs in the presence of Mg^{2+}. As for Mn^{2+} ions, we failed to study the BP interactions with them because of the paramagnetic nature of manganese.

Figure 2.

2. 5. Studies of the inhibition mechanism

The kinetic studies for the evaluation of the inhibition type were performed with compounds **2a** (group II) and **2c** (group I). We studied the dependence of the initial rate of the 3'-processing reaction vs the DNA substrate concentration at varied inhibitor concentrations in the presence of Mg^{2+} or Mn^{2+} ions. The results are given as double-reciprocal plots (Fig. 3).

First, we studied this dependence for compound **2a** in the presence of Mg^{2+} ions. As is seen in Fig. 3A, an increase in the compound **2a** concentration practically did not affect the maximal rate of the reaction (V_{max}) but caused an increase in the apparent Michaelis constant (K_m). This implies that in general the interaction of compound **2a** with IN follows the mechanism of *competitive inhibition*, i.e., the inhibitor binds to and competes with the substrate in the enzyme active site. Based on this model, the calculated values of the Michaelis constant K_m and inhibition constant K_I were determined as 12+/-6 nM and 38+/-8 μM, respectively, for the IN inhibition by compound **2a** in the presence of Mg^{2+} ions.

Figure 3.

For compound **2c** these dependences were shown to have another shape (Fig. 3B). In the presence of Mg^{2+} ions an increase in the inhibitor concentration resulted in the reduction of the V_{max}, whereas K_m did not change. This mode corresponds to the *noncompetitive inhibition*, i.e., the inhibitor binds to IN at the site differing from the substrate binding site. Based on the calculated K_m value (see above), the value of the inhibition constant K_I was found 2.0+/-0.5 μM.

In the case of Mn^{2+} ions the dependences of the 3'-processing initial rate vs the DNA substrate concentration at varied inhibitor concentrations were similar and supported the *noncompetitive mechanism* for both inhibitors (Figs. 3C and D). According to this model the calculated inhibition constants for compounds **2a** and **2c** were 4.4+/-0.8 and 1.0+/-0.3 μM, respectively.

Thus, the study of the dependence of the reaction initial rate vs the DNA substrate concentration at varied inhibitor concentrations demonstrated that the mechanism of IN inhibition for group II BPs (compound **2a**) changes from competitive to noncompetitive with the cofactor change from Mg^{2+} to Mn^{2+}, whereas group I BP (compound **2c**) always inhibited IN by the noncompetitive mechanism.

2.6. The BP effect on the IN-DNA binding

Upon the competitive inhibition the inhibitor competes with the substrate for the binding in the enzyme active site. Based on this principle we assumed that the group II inhibitors (compounds **2a**, **2b**, **2d**, and **5)** would prevent the formation of the IN-DNA complex in the presence of Mg^{2+} ions. Upon the noncompetitive inhibition, which was observed for all the tested BP in the presence of Mn^{2+} ions, the inhibitor bound to the enzyme at some other site and, therefore, is unlikely to have an impact upon the formation of the enzyme-substrate complex.

We studied the influence of the inhibitors of both groups on the complex formation of the IN with the U5 substrate in the presence of ions of both metals in the direct experiment using the DRaCALA (Differential Radial Capillary Action of Ligand Assay) approach [37]. Since this method was not previously used for characterizing the IN-DNA binding, first we evaluated its applicability for this purpose. To this end, we determined the dissociation constant, K_d, of the IN-DNA complex, (Fig. 4A). The calculated value of 20+/-6 nM, was close to that earlier found for the IN-DNA complex by the methods of gel shift[38] and fluorescence anisotropy change [39] . Thus, the DRaCALA method was proved to be useful for studying the IN-DNA binding.

As we suggested, none of the tested BP affected the formation of the IN-DNA complex in the presence of Mn^{2+} ions (Table 1, column 2). In the presence of Mg^{2+} ions compounds **2a**, **2b**, **2d**, and **5**, but not **2c**, inhibited the IN binding to the substrate (Table 1, column 1). These results confirmed the previous conclusions about different types of inhibition for group I and II BPs in the presence of Mg^{2+} ions and the change of the mechanism upon the Mg^{2+} replacement by Mn^{2+}. However, it is noteworthy that the inhibition of DNA binding was observed at higher BP concentrations than the inhibition of the IN catalytic activity (Table 1, columns 1, 3, and 5). This can probably be explained by the fact that the DRaCALA method only allows the evaluation of overall DNA-IN binding including both the substrate-specific and nonspecific

binding and, hence, we can only study the effect of the inhibitor in total. The inhibitor concentrations, at which they inhibit the formation of the specific IN-substrate complex, can be lower than those found by us and can be closer to those, at which they inhibit the 3'-processing and strand transfer reactions.

2.7. The inhibitor effect on the IN activity within the LEDGF complex

With the goal of further studying the mechanism of the IN inhibition with BP derivatives we tested the activity of these compounds toward the pre-formed IN-LEDGF complex composed of four IN and two LEDGF molecules [40]. Previously we demonstrated that the efficiency of the IN inhibition with a competitive inhibitor derived from a dimeric bisbenzimidazole reduced in the presence of LEDGF [41]. For the BPs tested, we found that group II compounds (**2a**, **2b**, and **2d**) did not inhibit IN within the IN-LEDGF complex in the presence of Mg^{2+} ions up to concentrations of 250 μM (Table 1, column 7). In the presence of Mn^{2+} ions they inhibited the complex with a similar efficiency as IN alone (Table 1, columns 4 and 8). As for compound **2c,** its inhibitory activity toward IN alone and IN-LEDGF complex was similar in the presence of both ions. These results supported once again the hypothesis on different mechanisms of IN inhibition by the tested BP derivatives.

Since competitive inhibitors compete with the substrate for the enzyme binding, the inability of compounds **2a**, **2b**, and **2d** to inhibit the IN-LEDGF complex can be explained by kinetic or thermodynamic factors, that is, faster or tighter binding of the DNA substrate to IN within its complex with LEDGF than to the free IN. The study of the strength of the DNA-IN-LEDGF complex in the presence of Mg^{2+} ions showed that K_d of this complex was 25+/-10 nM, which is comparable with the K_d value for the DNA-IN complex (Fig. 4A). We also calculated the rate of the DNA binding to IN and the IN-LEDGF complex using the DRaCALA method (Fig. 4B). The initial rate of the DNA binding to the complex (V_o 3.0 nM/min) was found to be considerably higher than that of the binding to IN (V_o = 0.7 nM/min).

Thus, the lack of activity of inhibitors of group II toward the IN-LEDGF complex can be explained by kinetic factors: the DNA binds to the complex faster than the inhibitor does. In the case of free IN the situation is inverse.

Figure 4.

2.7. Inhibition of IN mutants with increased resistance toward strand transfer inhibitors

All the experiments performed imply that compounds of groups I and II followed different mechanisms while inhibiting IN, that is, they are likely to bind to the enzyme in different modes. In order to find out their binding sites, we tested their activities toward IN preparations bearing E92Q, E138K, G140S, and N155H mutations that are known to affect the binding to IN of such inhibitors as *L*-chicoric acid, diketoacid L-731,988, raltegravir, elvitegravir, and dolutegravir, a second generation INSTI [7],[42],[43]. For these experiments we also used compounds **2a** and **2c** and Mg^{2+} ions, i.e., the conditions under which different mechanisms are involved and, hence, binding to IN occurs at different sites. However, both compounds inhibited the 3'-processing catalyzed by all of the mutants and wild type IN with a similar efficacy: in all the cases IC_{50} was 35+/-7 μM for compound **2a** and 7+/-2 μM for compound **2c.** These results demonstrated that the character of the BP binding to IN differed from that of the known inhibitors, but unfortunately they were useless for specifying the binding sites.

3. Discussion and Conclusions

The interest in BPs is stimulated by their capacity to inhibit the pyrophosphorolytic activity of HIV-1 reverse transcriptase and thus reduce the susceptibility of drug-resistant virus strains to azidothymidine [44]. We demonstrated that BPs could also inhibit another HIV-1 enzyme, integrase. The SAR analysis of the BP anti-integrase activity showed that these compounds must contain a chlorobenzyl residue as an R substituent for being effective IN inhibitors (Fig. 1). Substituents with other halogen atoms were not studied in the present work, and we cannot rule out their positive effect on the inhibitory activity of BPs. Of note, a halogen-containing aromatic substituent is a mandatory structural element of many of the IN inhibitors, but the halogen role is still unclear. A reason for the increased activity of halogen-containing inhibitors may be the formation of halogen bonding[45],[46]. This noncovalent interaction formed by the halogen atom and the nucleophile containing a lone electron pair is similar to the hydrogen bonding in both the properties and the way of formation.

For some enzymes it was found that a significant increase in the activity of their inhibitors was a result of the formation of halogen-bonded complexes [47],[48],[49]. Chlorine, bromine, and iodine atoms, but not the fluorine one, which possesses specific properties [50] can be involved in the formation of halogen bonds [45],[49]. Therefore, it is likely that the inhibitory activity of BPs with a chlorobenzyl substituent can be explained by the halogen bonding formation, which stabilizes the IN-inhibitor complexes.

Also, we found that the X substituent has an impact on the IN inhibition mechanism. In the presence of Mg^{2+} ions the inhibition mechanism of BP **2c** with X = NH_2 (group I) differs from that of all other BP (group II). This fact indirectly indicates that the group I and II

compounds bind to the enzyme using different modes (probably, at different binding sites). We assume that the reason for the different behavior of group I and II compounds may be the difference in their electron structures. Indeed, the ^{1}H NMR spectra indicated different distribution of the electron density in the hydrocarbon backbone of these compounds. The ^{31}P NMR spectra demonstrated that the P-C-P backbone of the group II inhibitors did not coordinate Mg^{2+} ions, whereas in the case of compound **2c** such coordination occurred with the efficacy that is growing with an increase in the amino group deprotonation degree.

Although currently it is difficult to detect directly the differences in the BP-IN binding, our results support further studies of BPs as IN inhibitors. Among all the compounds studied, α-amino BPs (analogues of compound **2c**) may be of the greatest interest, since, being IN noncompetitive inhibitors, they may inhibit the IN functioning in the preintegration complex. It is also essential that BP-based inhibitors are active toward IN mutants resistant to several known INSTI.

4. Experimental protocols

Materials and Methods

The structures of 17 bisphosphonates studied are shown in the Figure 1.

All reagents used were purchased from Aldrich or Acros Organics.

The acyl halides used in **Method C** were prepared by refluxing the corresponding acids with 2 eq of $SOCl_2$ in dry dichloromethane for 3-4 hours followed by vacuum distillation to give 75–88% of the target compounds.

The pyridinium acetic acids or acetonitriles were prepared reacting the corresponding pyridines with bromoacetic acid or bromoacetonitrile. For details see SI.

Flash chromatography was performed on Kieselgel (40-63 μm, Merck, Germany).

The inhibitor concentrations were measured by ^{1}H NMR using the known concentrations of *tert*-butanol-d1 in D_2O as an internal reference standard (relaxation delay (D1) was set to 60 s for ^{1}H measurements).

High-resolution electrospray mass spectra were obtained on Applied Biosystems/MDS Sciex QSTAR XL. NMR spectra were recorded on 400 MHz (^{1}H), 161.9 MHz (^{31}P), and 100.6 MHz (^{13}C) AMX III -400 Bruker spectrometer. Chemical shifts are reported in parts per million (ppm) using tetramethylsilane (^{1}H), *tert*-butanol-d1 (^{13}C), and 85% H_3PO_4 (^{31}P) as external standards. ^{13}C and ^{31}P NMR spectra were proton-decoupled unless otherwise specified.

Method A.

A mixture of carboxylic acid (2 mmol) or nitrile (2 mmol), phosphorous acid (2 mmol) and methanesulfonic acid (5 mL) in dry benzene (10 mL) was refluxed for 10-20 min till the mixture became homogenous. On cooling to 60-65 °C a solution of $POCl_3$ (3 mmol) in dry benzene (10 mL) was added dropwise for 30 min, maintaining the temperature below 70°C. The reaction mixture was refluxed with stirring for addition 8-12 h (24 h for (**3b**)), then the viscous yellowish mixture was cooled to ~40°C and pooled into the ice-cooled 3 N HCl (50 mL) under vigorous stirring followed by the reflux for 2 h. The aqueous layer was separated, concentrated *in vacuo* to a volume of 3 mL and kept for 12-24 h at +5°C till the bisphosphonates **3a-e**, **1d**, **2c** were crystallized. For BPs **1a-c**, the pH of the water layer was first adjusted to 4 with 50% NaOH and then kept for 5-12 h at +5°C for crystallization.

Method B.

Vinylidenediphosphonic acid.

VDPA was prepared by thermal dehydration of tetrasodium salt of etidronic acid followed by partial deionization of tetrasodium VDPA by CO_2 gas. Sodium bicarbonate formed was removed by filtration. For details and NMR data see SI.

Synthesis of 2-amino-1,1-bisphosphonates 4a-4c.

A water solution of disodium VDPA (1 eq) in water and the corresponding amine (1.5 eq) was concentrated *in vacuo* to homogenous syrup and heated at 120°C for 3 h. The reaction mixture was poured into a 50% water/ethanol mixture, acidified with HCl to pH 1 and allowed to crystallize at +5°C. The precipitated zwitterionic BPs were of 95% purity according to ^{1}H, ^{13}C, and ^{31}P NMR data.

Method C.

A solution of acyl chloride (3 mmol) in dry benzene (10 mL) was added dropwise at 0°C to triethylphosphite (3 mmol) in dry benzene (10 mL) under vigorous stirring and followed by stirring for additional 2 h at +5°C. Diethylphosphite (3 mmol) and diisopropyl amine (0.3 mmol) were added and stirring was continued for 4–5 h at+5°C. Reaction mixture was concentrated *in vacuo* and **2a**, **2b** were purified by column chromatography on silica gel with $CHCl_3$-MeOH (0 to 15% MeOH) as an eluent. Solvents were removed *in vacuo* and ethyl groups were routinely removed by using 5 equivalents of TMSBr overnight at rt followed by methanolysis.

Method D.

To a solution of 1.2 mL (4 mmol) tetraisopropyl methylenebisphosphonate in dry THF (5 mL) 160 mg (4 mmol) of NaH (60% suspension in oil) in of dry THF (5 mL) was added at 0°C with stirring under the Ar atmosphere and stirring was continued for 1 h at 0°C, and then for 3 h at rt. A solution of 782 mg (4 mmol) 3,4-dichlorobenzyl chloride in THF (5 mL) was added to the resulted carbanion solution and stirred overnight at rt. The reaction was quenched with saturated NH_4Cl (20 mL), extracted with DCM (3x50 mL), dried (Na_2SO_4) and concentrated *in vacuo*. Target BPs **2d** or **5** were purified by column chromatography on silica gel eluting with EtOAc – MeOH gradient (0 to 25% MeOH). For bisphosphonate **5** 10 mmol NaH and 10 mmol 3,4-dichlorobenzylchloride were used. Tetraisopropyl esters were refluxed with 48% HBr (4 mL) for 2 h followed by co-evaporation with water (3x15 mL) and drying *in vacuo* over P_2O_5/KOH to give target **2d** and **5** as vaxi oils.

1-Hydroxy-2-phenylethylidene-1,1-bisphosphonic acid (1a). Compound **1** was prepared from phenylacetic acid following **Method A** as colorless solid (disodium salt, 490 mg, 75%). ^{1}H NMR (D_2O, pH 1): δ 7.38-7.28 (m, 5H), 3.32 (t, J_{PH} = 14 Hz, 2H). ^{31}P (D_2O, pH 1): δ 19.0 s; lit. 19.0 s[16]. ^{13}C (D_2O, pH 2, *t*-BuOD 30.3 ppm): δ 7.48-7.36 (5H, m, Ph), 74.0 (t, J_{PC} = 147.0 Hz), 40.6 s

Compound **1b** was available from previous work [17]

1-Hydroxy-5-phenylpentylidene-1,1-bisphosphonic acid (1c). Compound **1c** was prepared from phenylpentanoic acid following **General Method A** as colorless solid (tetrapotassium salt, 391 mg, 41%). ^{1}H NMR (D_2O, pH 2):δ 7.35-7.20 (m, Ph, 5H), 2.63 (t, J = 7.1 Hz, CH_2-PCP, 2H), 2.08-1.96 (m, CH_2-PCP, 2H), 1.66-1.57 (m,-$(CH_2)_2$-, 4H). ^{31}P (D_2O, pH 2):δ 18.5 s. ^{13}C (D_2O, pH 2, *t*-BuOD 30.3 ppm): δ 144.4 s, 129.6 s, 126.8 s, 74.1 t (J_{PC} = 147 Hz), 35.2 s, 33.9 s, 32.0 s, 30.1 s.

1-Amino-2-phenylethylidene-1,1-bisphosphonic acid (1d). Compound **1d** was prepared from phenylacetonitrile following **Method A** as colorless solid (180 mg, 32%). ^{1}H NMR (D_2O, pH 3): δ 7.46-7.32 (5H, m, Ph), 3.43 (2H, t, J_{PC} = 12.5 Hz, CH_2-PCP).^{31}P NMR (D_2O, pH 6, P-H coupled) δ 12.4 (t, J_{PH} = 12 Hz). ^{31}P NMR (D_2O, pH 2) δ 12.3 s. ^{13}C NMR (D_2O, pH 14, *t*-BuOD 30.3 ppm): δ 141.9 s, 133.3 s, 128.6 s, 126.8 s, 58.5 (t, J_{PC} = 129.4 Hz), 41.2 s.

1-Hydroxy-2-(3,4-dichlorophenyl)ethylidene-1,1-bisphosphonic acid (2a). Compound **2a** was prepared from 3,4-dichlorophenylacetic acid following **Method C** as colorless solid (750 mg,

71%). ^{1}H NMR (D_2O+25% DMSO-d6, pH 2): δ 7.39 (d, *J* 1.4 Hz, 1H), 7.28 (d, *J* 8.3 Hz, 1H), 7.15 (dd, *J* = 8.3 Hz, 1.4 Hz, 1H), 3.11 (t, J_{PH} = 13 Hz, 2H). ^{13}C NMR (D_2O+25% DMSO-d6, pH 2, *t*-BuOD 30.3): δ 132.5 s, 131.8 s, 131.1 s, 130.8 s, 74.3 (t, J_{PC} = 147.2 Hz), 38.3 s. ^{31}P NMR (D_2O, pH 2): δ 18.0 s

1-Hydroxy-2-(4-chlorophenyl)ethylidene-1,1-bisphosphonic acid (2b). Compound **2b** was prepared from 4-chlorophenylacetic acid following **Method C** as colorless solid (785 mg, 82%). ^{1}H NMR (D_2O, pH 5): δ 7,37 (d, *J* = 8.4 Hz), 7,28 (d, *J* = 8.4 Hz), 3,23 (t, *J* = 12.6 Hz).^{13}C NMR (D_2O, pH 12, *t*-BuOD 30.3 ppm): δ 134.1 s, 132.3 s, 131.5 s, 129.5 s, 74.0 (t, J_{PC} = 147 Hz), 38.9 s. ^{31}P NMR (D_2O, pH 5): δ 18.0 s. HREIMS: m/z 314.9594 (calcd for $C_8H_{10}ClO_7P_2$, [M-H]+314.9590).

1-Amino-2-(3,4-dichlorophenyl)ethylidene-1,1-bisphosphonic acid (2c). Compound **2c** was prepared from 3,4-dichlorophenylacetonitrile following **Method A** as colorless solid (273 mg, 39%). ^{1}H NMR (D_2O, pH 11): δ 7.55 (d, *J* = 2 Hz, 1H), 7.39 (d, *J* = 8.3 Hz, 1H), 7.30 (dd, *J* = 8.3, *J* = 2 Hz, 1H), 3.16 (t, *J* = 12 Hz, 2H). ^{13}C NMR (D_2O, pH 11, DMSO-d6 39.52 ppm): δ 140.4 s, 134.4 s, 132.8 s, 131.9 s, 130.9 s, 130.6 s, 57.5 (t, J_{PC} = 123.6 Hz), 40.3 s ^{31}P NMR (D_2O, pH 11): δ 18.9 s. HREIMS: m/z 347.9366 (calcd for $C_8H_{10}Cl_2NO_6P_2$, [M-H]+ 347.9360).

2-(3,4-dichlorophenyl)ethylidene-1,1-bisphosphonic acid (2d). Compound **2d** was prepared from 3,4-dichlorobenzylchloride following **Method D** as colorless solid (disodium salt, 379 mg, 50%). ^{1}H NMR (D_2O, pH 10): δ 7.53 (s, 1H), 7.40 (d, *J* = 8.2 Hz, 1H), 7.27 (dd, J_1 = 8.2 Hz, J_2 = 2 Hz 1H), 3.06 (ddd, J_{HH} = 7 Hz, J_{PH} = 15 Hz, 2H), 2.10 (dt, J_{HH} = 7 Hz, J_{PH} = 20 Hz, 1H). ^{13}C NMR (D_2O, pH 10, *t*-BuOD 30.3 ppm): δ 157.3 s, 138.6 s, 126.1 s, 125.2 s, 124.3 s, 36.8 (t, J_{PC} = 111 Hz), 26.4 s. ^{31}P NMR (D_2O, pH 10): δ 19.4 s. HREIMS: m/z 332.9265 (calcd for $C_8H_9Cl_2O_6P_2$, [M-H]+332.9251).

1-Hydroxy-2-(pyridine-1-yl)ethylidene-1,1-bisphosphonic acid (3a). Compound **3a** was prepared from 2-(pyridine-1-yl)acetic acid following **Method A** as colorless solid (449 mg, 79%). ^{1}H NMR (D_2O, pH 1): δ 8.9 (d, *J* = 6 Hz, 2H), 8.6 (t, *J* = 8 Hz, 1H), 8.0 (t, *J* = 7Hz, 2H), 5.0 (t, *J* = 9.5 Hz). ^{13}C NMR (D_2O, pH 1, acetone 30.9 ppm): δ 146.7 s, 127.6 s, 73.4 (t, *J* = 137 Hz, PCP), 64.4 s (CH_2). ^{31}P NMR (D_2O, pH 1): δ 14.4 s; lit. 14.3 s [20]

1-Amino-2-(pyridine-1-yl)ethylidene-1,1-bisphosphonic acid (3b). Bisphosphonate **3b** was prepared by **Method A** from 2-(pyridine-1-yl)acetonitrile (synthesized as described in SI) as colorless solid (221 mg, 39%). ^{1}H NMR (D_2O, pH 1): δ 9.0 (d, *J* = 5.9 Hz, 2H), 8.7 (t, *J* = 7.8 Hz, 1H), 8.1 (t, *J* = 6.7 Hz, 2H), 5.2 (t, J_{PH} = 9.5 Hz). ^{13}C NMR (D_2O, pH 1): δ 146.9 (s, Py), 146.0 (s, Py), 127.7 (s, Py), 61.5 (s, CH_2), 57.1 (t, J_{PC} = 123 Hz, PCP). ^{31}P NMR (D_2O, pH 1): δ 8.5 s. ^{31}P NMR (D_2O, pH 14): δ 17.4 s

1-Hydroxy-2-(4-phenylpyridine-1-yl)ethylidene-1,1-bisphosphonic acid (3c). Bisphosphonate **3c** was prepared by **Method A** from 2-(4-phenylpyridine-1-yl)acetic acid (synthesized as described in SI) as colorless solid (526 mg, 73%).

^{1}H NMR (D_2O, pH 1): δ 8.8 (d, J = 6.3 Hz, 2H, Py), 8.2 (d, J = 6.3 Hz, 2H, Py), 7.9 (d, J = 6.6 Hz, 2H, Ph), 7.6 (m, 3H, Ph), 5.0 (t, J_{PH} = 9.5 Hz). ^{13}C NMR (D_2O, pH 1): δ 159.9 (s, Py), 148.9 (s, Py), 137.0 (s, Py), 135.1 (s, Ph), 132.6 (s, Ph), 131.0 (s, Ph), 126.8 (s, Ph), 76.1 (t, J_{PC} = 134 Hz, PCP), 66.2 (s, CH_2). ^{31}P NMR (D_2O, pH 1): δ 14.9 s (lit. 14.7 s [21])

1-Hydroxy-2-(3-hydroxypyridine-1-yl)ethylidene-1,1-bisphosphonic acid (3d). Bisphosphonate **3d** was prepared by **Method A** from 2-(3-hydroxypyridine-1-yl)acetic acid (synthesized as described in SI) as colorless solid (282 mg, 47%). ^{1}HNMR (D_2O, pH 14): δ 7.8 (d, J = 5.6 Hz, 1H), 7.8 (s, 1H), 7.3 (m, 2H), 4.6 (t, J = 9 Hz, 2H). ^{13}CNMR (D_2O, pH 10, acetone 30.9 ppm): δ 164.6 (s, Py), 136.1 (s, Py), 133.2 (s, Py), 130.6 (s, Py), 126.0 (s, Py), 73.8 (t, J_{PC} = 127 Hz, PCP), 64.5 (s, CH_2). ^{31}P NMR (D_2O, pH 14): δ 15.5 s

1-Hydroxy-2-(2-ethylpyridine-1-yl)ethylidene-1,1-bisphosphonic acid (3e). Bisphosphonate **3e** was prepared by **Method A** from 2-(2-ethylpyridine-1-yl) acetic acid (synthesized as described in SI) as colorless solid (319 mg, 51%).

^{1}H NMR (D_2O, pH 1): δ 8.8 (dd, J_1 = 6.4 Hz, J_1 = 1.6 Hz, 1H, Py), 8.3 (ddd, J_1 = 8.0 Hz, J_2 = 1.7 Hz, 1H, Py), 7.8 (dd, J_1 = 8.0 Hz, J_2 = 1.8 Hz, 1H, Py), 7.7 (ddd, J_1 = 6.4 Hz, J_2 = 1.7 Hz, 1H, Py), 5.0 (t, J_{HP} = 10 Hz, 2H, N-CH_2), 3.3 (q, J = 7.5 Hz, 2H, CH_2-Et),1.27 (t, J = 7.5 Hz, 3H, CH_3). ^{13}CNMR (D_2O, pH 10): δ 161.0 (s, Py), 146.7 (s, Py), 144.3 (s, Py), 126.4 (s, Py), 123.0 (s, Py), 73.8 (t, J_{PC} = 126 Hz, PCP), 59.1 (s, CH_2-Py), 26.1 (s, $\underline{CH_2}$-CH_3), 11.2 (s, CH_3). ^{31}P NMR (D_2O, pH 10): δ 15.3 s. ^{31}P NMR (D_2O, pH 10, coupled): δ 15.3 (t, J_{PH} = 10 Hz)

(2-Phenylethylamino)-2-ethylidene-1,1-bisphosphonic acid (4a). Compound **4a** was prepared from 3.78 mL (30 mmol) 2-phenylethylamine and VDPA (20 mmol) following **Method B** as colorless solid (4.3 g, 69%, as calculated for VDPA). ^{1}H NMR (D_2O, pH 9): δ 7.39-7.27 (5H, m, Ph), 3.35 (dt, J_{HH} = 6.5 Hz, J_{PH} = 15 Hz, 2H, CH_2-PCP), 3.27 (t, J = 7.5 Hz, 2H, CH_2-$\underline{CH_2}$-NH), 2.98 (t, J = 7.5 Hz, 2H, CH_2-Ph), 2.07 (tt, J_{HH} = 6.5 Hz, J_{PH} = 20 Hz, 1H, H-PCP). ^{31}P NMR (D_2O, pH 9): δ 16.2 s. ^{13}C NMR (D_2O, pH 9, *t*-BuOD 30.3ppm):δ 137.3 s, 129.6 s, 129.5 s, 127.8 s, 48.6 s, 47.2 s, 37.5 (t, J_{PC} = 110 Hz)

Phenylamino-2-ethylidene-1,1-bisphosphonic acid (4b)

Compound **4b** was prepared from 2.7 mL (30 mmol) freshly distilled aniline and VDPA (20 mmol) following **Method B** as colorless solid becoming brownish if kept on air (4.1 g, 73%, as calculated for VDPA). ^{1}H NMR (D_2O, pH 2):δ 7.51-7.42 (5H, m, Ph), 3.35 (2H, ddd, J_{HH} 7.5 Hz, J_{PH} 15Hz, J_{PH} 13Hz, CH_2-PCP), (1H, tt, J_{HH} = 7.5 Hz, J_{PH} = 21 Hz, H-PCP). ^{13}C NMR (D_2O, pH

2, *t*-BuOD 30.3 ppm) : δ 134.9 s, 131.0 s, 130.9 s, 130.6 s, 123.1 s, 50.2 s (CH_2), 36.3 (t, J_{CP} = 121 Hz). ^{31}P NMR (D_2O, pH 2):δ 15.8 s

((4-Iodophenyl)amino)-2-ethylidene-1,1-bisphosphonic acid (4c). To a solution of 562 mg (2 mmol) bisphosphonate **4b** in 1M $NaHCO_3$ (10 mL) 762 mg (3 mmol) of iodine was addad and resulted mixture was stirred overnight at 5°C followed by the addition of 126 mg (1 mmol) Na_2SO_3. The resulted solution was applied on a column of Dowex-50 (H^+) resin (50 mL) then column was washed with 50 mL of water and combined eluents were concentrated *in vacuo* to 5 mL and kept at +5°C for crystallization (635 mg, 78%). ^{1}H NMR (D_2O, pH 10): δ 7.5 (d, *J* = 9 Hz, 2H), 6.6 (d, *J* = 9 Hz, 2H), 3.5 (ddd, J_{HH} = 7 Hz, J_{PH} = 14 Hz, 2H), 2.1 (dt, J_{HH} = 7 Hz, J_{PH} = 20.5 Hz, 1H). ^{31}P NMR (D_2O, pH 10): δ 18.5 s. ^{31}P NMR (coupled): δ 18.5 (dt, J_1 = 14 Hz, J_2 = 20.5 Hz). ^{13}C NMR: δ (D_2O, pH 7, *t*-BuOD 30.3 ppm): δ 147.9 s, 138.5 s. 117.7 s, 79.8 s, 41.9 s, 39.2 (t, *J* = 114.2 Hz). HREIMS: m/z 405.9150 (calcd for $C_8H_{11}INO_6P_2$, [M-H]+ 405.9106).

Bis-(2-(3,4-dichlorophenyl)ethylidene)-1,1-bisphosphonic acid (5). Compound **5** was prepared from 3,4-dichlorobenzylchloride following **Method D** as colorless solid (tetra potassium salt, 1.1 g, 92%). ^{1}H NMR (D_2O, pH 12): δ 7.64 (s, 2H), 7.48 (d, *J* = 8.2 Hz, 2H), 7.33 (d, *J* = 8.2 Hz, 2H), 3.02 (t, *J* = 15.4 Hz, 4H). ^{13}C NMR (D_2O, pH 12, *t*-BuOD 30.3 ppm): δ 158.1 s, 139.0 s, 126.9 s, 125.2 s, 125.1 s, 36.8 (t, J_{PC} = 112 Hz), 26.0 s. ^{31}P NMR (D_2O, pH 12): δ 20.9 s. HREIMS: m/z 490.8942 (calcd for $C_{15}H_{13}Cl_4O_6P_2$, [M-H]+490.8942).

Biology

The detergent-free recombinant IN protein (wt and mutant forms) was produced in *Escherichia coli* and purified as previously described[51]. The plasmids containing the mutant forms of the IN genes (E92Q, E138K, G140S, and N155H substitutions) were obtained by site-directed mutagenesis of a plasmid encoding wild-type IN using the QuikChange II Site-Directed Mutagenesis kit (Agilent Technologies, USA). All procedures were performed in accordance with the manufacturer's instructions.

IN/LEDGF complex was produced as described in [40].

All oligonucleotides were synthesized by the phosphoramidite method on an automatic ABI 3400 DNA synthesizer (Applied Biosystems, USA) under conditions recommended by manufacturer and purified by electrophoresis in a 20% polyacrylamide/7 M urea gel.

^{32}P-labeled IN substrate preparation. DNA duplexes consisting of oligonucleotides U5A (5'-ACTGCTAGAGATTTTCACAC-3') and U5B (5'-GTGTGGAAAATCTCTAGCAGT-3') or U5B-2 (5'-GTGTGGAAAATCTCTAGCA-3'), and mimicking the end of the HIV-1 U5 LTR were used as IN substrates. The U5B or U5B-2 oligonucleotide (10 pmol) was labeled with T4 polynucleotide kinase (Fermentas, Lithuania) and 50 μCi [γ^{32}P]ATP (3000 Ci/mmol). After 1 h of incubation at 37°C, the T4 polynucleotide kinase was inactivated by the addition of EDTA followed by heating at 65°C for 5 minutes. The U5B or U5B-2 oligonucleotide was then annealed with an equimolar amount of complementary oligonucleotide, U5A. The resulting U5B/U5A or U5B-2/U5A duplex was then purified from unincorporated [γ-^{32}P]ATP by centrifugation through MicroSpin G-25 Columns (GE Healthcare, UK).

Inhibition of 3'-processing and strand transfer reactions. ^{32}P-labeled duplex U5B/U5A (3 nM) for 3'-processing or U5B-2/U5A (10 nM) for strand transfer was incubated with IN (100 nM) in 20 μl of the buffer A (20 mM HEPES pH 7.2, 7.5 mM $MgCl_2$ or $MnCl_2$, 1 mM DTT) in the presence of increasing concentrations of an inhibitor at 37°C for 2 h. The reaction was stopped by adding 80 μl of stop solution (7 mM EDTA, 0.3 M sodium acetate, and 10 mM Tris–HCl, pH 8). IN was extracted with 100 μl of phenol–chloroform–isoamyl alcohol mixture (25:24:1). DNA was precipitated with 250 μl of ethanol at 0°C and assayed by denaturing PAGE (20%). Gel was visualized in a STORM 840TM Phosphorimager (Molecular Dynamics, United States). The reaction efficiency was assessed using the Image QuaNTTM 4.1 program.

Inhibition of 3' processing catalyzed by the complex IN/LEDGF was studied analogously using 100 mM IN combined with 50 nM LEDGF.

For the inhibition mechanism studies, IN (100 nM) was incubated with ^{32}P-labeled substrate U5B/U5A (2.5–12.5 nM) and compound **2a** (0–39 μM) or **2c** (0–15 μM), in 20 μl of the buffer A for 1 h at 37°C.

DNA binding assay. The ^{32}P-labeled substrate U5B/U5A (3 nM) was incubated with HIV-1 IN at different concentrations (3 – 300 nM) in 10 μl of the buffer A at 25°C for 20 min before loading on nitrocellulose membrane (Amersham Hybond, GE Healthcare). Molecular Dynamics STORM 840 Phosphorimager was used for analysis and quantification.

For kinetic measurements, the ^{32}P-labeled substrate U5B/U5A (3 nM) was incubated with IN alone (100 nM) or combined with LEDGF (50 nM) in 10 μl of the buffer A at 25°C, and the aliquots were taken after different times of incubation (0-60 min).

To study the DNA-IN binding inhibition, compounds **2a-d** or **5** (0-500 μM) were added to the DNA/IN mixture.

Abbreviations:

HAART - highly active antiretroviral therapy, , IN – integrase, BP – bisphosphonate, INSTI – integrase strand transfer inhibitor, LEDGF - lens epithelium derived growth factor, RT - reverse transcriptase, VDPA – vinylidenediphosphonic acid. DRaCALA - differential radial capillary action of ligand assay

ACKNOWLEDGEMENTS

We thank Dr. Janne Weisell from the University of Eastern Finland for providing HREIMS data and Dr. Alex Khomutov from Engelhardt Institute of Molecular Biology RAS (Moscow, Russia) for his thoughtful comments on the manuscript. The work was supported by the Russian Foundation for the Basic Research (projects 13-04-91440, 11-04-01586, 12-04-00958) and by the Presidium of the Russian Academy of Sciences (Programme “Molecular and Cellular Biology”) and by the Academy of Finland (Grant No 132070), strategic funding of UEF and PhoSciNet COST action.

Supporting Information Available:

^{1}H, ^{13}C, ^{31}P NMR data for all new and most other BPs. Detail synthetic procedures for preparation some intermediate compounds. Supplementary data associated with this article can be found in the online version, at http://dx.doi.org/

REFERENCES

[1] P.K. Quashie, R.D. Sloan, M.A. Wainberg, Novel therapeutic strategies targeting HIV integrase, BMC Med, 10 (2012) 34.
[2] C. Marchand, K. Maddali, M. Metifiot, Y. Pommier, HIV-1 IN inhibitors: 2010 update and perspectives, Curr Top Med Chem, 9 (2009) 1016-1037.
[3] FDA approves raltegravir tablets, AIDS Patient Care STDS, 21 (2007) 889.
[4] FDA approves new 4-drug once-a-day HIV treatment, AIDS Policy Law, 27 (2012) 1.
[5] E. Serrao, S. Odde, K. Ramkumar, N. Neamati, Raltegravir, elvitegravir, and metoogravir: the birth of "me-too" HIV-1 integrase inhibitors, Retrovirology, 6 (2009) 25.
[6] M. Metifiot, C. Marchand, K. Maddali, Y. Pommier, Resistance to integrase inhibitors, Viruses, 2 (2010) 1347-1366.
[7] M.A. Wainberg, T. Mesplede, P.K. Quashie, The development of novel HIV integrase inhibitors and the problem of drug resistance, Curr Opin Virol, 2 (2012) 656-662.
[8] S.L. Karmon, M. Markowitz, Next-generation integrase inhibitors : where to after raltegravir?, Drugs, 73 (2013) 213-228.
[9] U. Pradere, V. Roy, A. Montagu, O. Sari, M. Hamada, J. Balzarini, R. Snoeck, G. Andrei, L.A. Agrofoglio, Synthesis and antiviral evaluation of bis(POM) prodrugs of (E)-[4'-phosphono-but-2'-en-1'-yl]purine nucleosides, Eur J Med Chem, 57 (2012) 126-133.
[10] D.G. Piotrowska, J. Balzarini, I.E. Glowacka, Design, synthesis, antiviral and cytostatic evaluation of novel isoxazolidine nucleotide analogues with a 1,2,3-triazole linker, Eur J Med Chem, 47 (2012) 501-509.
[11] M. Hamada, V. Roy, T.R. McBrayer, T. Whitaker, C. Urbina-Blanco, S.P. Nolan, J. Balzarini, R. Snoeck, G. Andrei, R.F. Schinazi, L.A. Agrofoglio, Synthesis and broad spectrum antiviral evaluation of bis(POM) prodrugs of novel acyclic nucleosides, Eur J Med Chem, 67 (2013) 398-408.
[12] L. Roux, S. Priet, N. Payrot, C. Weck, M. Fournier, F. Zoulim, J. Balzarini, B. Canard, K. Alvarez, Ester prodrugs of acyclic nucleoside thiophosphonates compared to phosphonates: synthesis, antiviral activity and decomposition study, Eur J Med Chem, 63 (2013) 869-881.
[13] C. Cruchaga, E. Anso, A. Rouzaut, J.J. Martinez-Irujo, Selective excision of chain-terminating nucleotides by HIV-1 reverse transcriptase with phosphonoformate as substrate, J Biol Chem, 281 (2006) 27744-27752.
[14] Y. Song, J.M. Chan, Z. Tovian, A. Secrest, E. Nagy, K. Krysiak, K. Bergan, M.A. Parniak, E. Oldfield, Bisphosphonate inhibitors of ATP-mediated HIV-1 reverse transcriptase catalyzed excision of chain-terminating 3'-azido, 3'-deoxythymidine: a QSAR investigation, Bioorg Med Chem, 16 (2008) 8959-8967.
[15] A. Anisenko, J. Agapkina, T. Zatsepin, D. Yanvarev, M. Gottikh, A new fluorometric assay for the study of DNA-binding and 3'-processing activities of retroviral integrases and its use for screening of HIV-1 integrase inhibitors, Biochimie, 94 (2012) 2382-2390.
[16] M. Lecouvey, I. Mallard, T. Bailly, R. Burgada, Y. Leroux, A mild and efficient one-pot synthesis of 1-hydroxymethylene-1,1-bisphosphonic acids. Preparation of new tripod ligands, Tetrahedron Letters, 42 (2001) 8475-8478.
[17] D.V. Yanvarev, A.N. Korovina, N.N. Usanov, S.N. Kochetkov, Non-hydrolysable analogues of inorganic pyrophosphate as inhibitors of hepatitis C virus RNA-dependent RNA-polymerase, Russ J Bioorg Chem, 38 (2012) 224-229.
[18] M. Fukuda, Y. Okamoto, H. Sakurai, Nonequivalence between the geminal dihydroxyphosphinyl groups in some 2-substituted 1-aminoethylidenedophosphonic acids, Chemistry Letters, 6 (1977) 529-532.
[19] J.H. No, F. de Macedo Dossin, Y. Zhang, Y.L. Liu, W. Zhu, X. Feng, J.A. Yoo, E. Lee, K. Wang, R. Hui, L.H. Freitas-Junior, E. Oldfield, Lipophilic analogs of zoledronate and

risedronate inhibit Plasmodium geranylgeranyl diphosphate synthase (GGPPS) and exhibit potent antimalarial activity, Proc Natl Acad Sci U S A, 109 (2012) 4058-4063.
[20] J.M. Sanders, Y. Song, J.M. Chan, Y. Zhang, S. Jennings, T. Kosztowski, S. Odeh, R. Flessner, C. Schwerdtfeger, E. Kotsikorou, G.A. Meints, A.O. Gomez, D. Gonzalez-Pacanowska, A.M. Raker, H. Wang, E.R. van Beek, S.E. Papapoulos, C.T. Morita, E. Oldfield, Pyridinium-1-yl bisphosphonates are potent inhibitors of farnesyl diphosphate synthase and bone resorption, J Med Chem, 48 (2005) 2957-2963.
[21] Y. Zhang, A. Leon, Y. Song, D. Studer, C. Haase, L.A. Koscielski, E. Oldfield, Activity of nitrogen-containing and non-nitrogen-containing bisphosphonates on tumor cell lines, J Med Chem, 49 (2006) 5804-5814.
[22] L. Deng, K. Endo, M. Kato, G. Cheng, S. Yajima, Y. Song, Structures of 1-Deoxy-D-Xylulose-5-Phosphate Reductoisomerase/Lipophilic Phosphonate Complexes, ACS Med Chem Lett, 2 (2011) 165-170.
[23] G.R. Kieczykowski, R.B. Jobson, D.G. Melillo, D.F. Reinhold, V.J. Grenda, I. Shinkai, Preparation of (4-Amino-1-Hydroxybutylidene)bisphosphonic Acid Sodium Salt, MK-217 (Alendronate Sodium). An Improved Procedure for the Preparation of 1-Hydroxy-1,1-bisphosphonic Acids, The Journal of Organic Chemistry, 60 (1995) 8310-8312.
[24] M.S. Marma, Z. Xia, C. Stewart, F. Coxon, J.E. Dunford, R. Baron, B.A. Kashemirov, F.H. Ebetino, J.T. Triffitt, R.G. Russell, C.E. McKenna, Synthesis and biological evaluation of alpha-halogenated bisphosphonate and phosphonocarboxylate analogues of risedronate, J Med Chem, 50 (2007) 5967-5975.
[25] M. Company, in, Great Britain, 1970, pp. 1-15.
[26] S.P. Korolev, Y.Y. Agapkina, M.B. Gottikh, Clinical Use of Inhibitors of HIV-1 Integration: Problems and Prospects, Acta Naturae, 3 (2011) 12-28.
[27] K. Ramkumar, K.V. Tambov, R. Gundla, A.V. Manaev, V. Yarovenko, V.F. Traven, N. Neamati, Discovery of 3-acetyl-4-hydroxy-2-pyranone derivatives and their difluoridoborate complexes as a novel class of HIV-1 integrase inhibitors, Bioorg Med Chem, 16 (2008) 8988-8998.
[28] H. Sharma, S. Patil, T.W. Sanchez, N. Neamati, R.F. Schinazi, J.K. Buolamwini, Synthesis, biological evaluation and 3D-QSAR studies of 3-keto salicylic acid chalcones and related amides as novel HIV-1 integrase inhibitors, Bioorg Med Chem, 19 (2011) 2030-2045.
[29] J. Agapkina, T. Zatsepin, E. Knyazhanskaya, J.-F. Mouscadet, M. Gottikh, Structure–Activity Relationship Studies of HIV-1 Integrase Oligonucleotide Inhibitors, ACS Medicinal Chemistry Letters, 2 (2011) 532-537.
[30] S. Hare, S.S. Gupta, E. Valkov, A. Engelman, P. Cherepanov, Retroviral intasome assembly and inhibition of DNA strand transfer, Nature, 464 (2010) 232-236.
[31] L. Krishnan, X. Li, H.L. Naraharisetty, S. Hare, P. Cherepanov, A. Engelman, Structure-based modeling of the functional HIV-1 intasome and its inhibition, Proc Natl Acad Sci U S A, 107 (2010) 15910-15915.
[32] E. Matczak-Jon, V. Videnova-Adrabińska, Supramolecular chemistry and complexation abilities of diphosphonic acids, Coordination Chemistry Reviews, 249 (2005) 2458-2488.
[33] E. Matczak-Jon, B. Kurzak, A. Kamecka, P. Kafarski, Interactions of zinc(II), magnesium(II) and calcium(II) with aminomethane-1,1-diphosphonic acids in aqueous solutions, Polyhedron, 21 (2002) 321-332.
[34] L.M. Salonen, M. Ellermann, F. Diederich, Aromatic rings in chemical and biological recognition: energetics and structures, Angew Chem Int Ed Engl, 50 (2011) 4808-4842.
[35] T. Appleton, J. Hall, A. Harris, H. Kimlin, I. McMahon, N.M.R. study of acid-base equilibria of aminoalkylphosphonic acids, $^{+}NH_3(CH_2)_nPO_3H^-$ (n = 1,2,3): Evidence for cyclization in solution, Australian Journal of Chemistry, 37 (1984) 1833-1840.
[36] C.T. Burt, H.M. Cheng, S. Gabel, R.E. London, ATP, ADP, and magnesium mixed solutions: in vitro 31P NMR characterization and in vivo application to lens, J Biochem, 108 (1990) 441-448.

[37] G.P. Donaldson, K.G. Roelofs, Y. Luo, H.O. Sintim, V.T. Lee, A rapid assay for affinity and kinetics of molecular interactions with nucleic acids, Nucleic Acids Res, 40 (2012) e48.
[38] M. Smolov, J. Agapkina, M. Buckle, J.F. Mouscadet, M. Gottikh, Characterization of DNA binding by HIV-1 integrase using Schiff-base formation, FEBS Journal, 272 (2005) 19-20.
[39] J. Agapkina, M. Smolov, S. Barbe, E. Zubin, T. Zatsepin, E. Deprez, M. Le Bret, J.F. Mouscadet, M. Gottikh, Probing of HIV-1 integrase/DNA interactions using novel analogs of viral DNA, J Biol Chem, 281 (2006) 11530-11540.
[40] F. Michel, C. Crucifix, F. Granger, S. Eiler, J.F. Mouscadet, S. Korolev, J. Agapkina, R. Ziganshin, M. Gottikh, A. Nazabal, S. Emiliani, R. Benarous, D. Moras, P. Schultz, M. Ruff, Structural basis for HIV-1 DNA integration in the human genome, role of the LEDGF/P75 cofactor, EMBO J, 28 (2009) 980-991.
[41] S.P. Korolev, V.N. Tashlitskii, M.A. Smolov, A.V. Gromyko, A.L. Zhuze, I. Agapkina, M.B. Gottikh, [HIV-1 integrase inhibition by dimeric bisbenzimidazoles having different spacers], Mol Biol (Mosk), 44 (2010) 718-727.
[42] I. Malet, O. Delelis, M.A. Valantin, B. Montes, C. Soulie, M. Wirden, L. Tchertanov, G. Peytavin, J. Reynes, J.F. Mouscadet, C. Katlama, V. Calvez, A.G. Marcelin, Mutations associated with failure of raltegravir treatment affect integrase sensitivity to the inhibitor in vitro, Antimicrob Agents Chemother, 52 (2008) 1351-1358.
[43] F. Ceccherini-Silberstein, I. Malet, R. D'Arrigo, A. Antinori, A.G. Marcelin, C.F. Perno, Characterization and structural analysis of HIV-1 integrase conservation, AIDS Rev, 11 (2009) 17-29.
[44] M.M. Prokofjeva, P.V. Spirin, D.V. Yanvarev, A.V. Ivanov, M.S. Novikov, O.A. Stepanov, M.B. Gottikh, S.N. Kochetkov, B. Fehse, C. Stocking, V.S. Prassolov, Screening of Potential HIV-1 Inhibitors/Replication Blockers Using Secure Lentiviral in Vitro System, Acta Naturae, 3 (2011) 55-65.
[45] P. Politzer, P. Lane, M.C. Concha, Y. Ma, J.S. Murray, An overview of halogen bonding, J Mol Model, 13 (2007) 305-311.
[46] P. Metrangolo, G. Resnati, H.H.D. Arman, Halogen Bonding: Fundamentals and Applications, Springer, 2008.
[47] L.A. Hardegger, B. Kuhn, B. Spinnler, L. Anselm, R. Ecabert, M. Stihle, B. Gsell, R. Thoma, J. Diez, J. Benz, J.M. Plancher, G. Hartmann, D.W. Banner, W. Haap, F. Diederich, Systematic investigation of halogen bonding in protein-ligand interactions, Angew Chem Int Ed Engl, 50 (2011) 314-318.
[48] L.A. Hardegger, B. Kuhn, B. Spinnler, L. Anselm, R. Ecabert, M. Stihle, B. Gsell, R. Thoma, J. Diez, J. Benz, J.M. Plancher, G. Hartmann, Y. Isshiki, K. Morikami, N. Shimma, W. Haap, D.W. Banner, F. Diederich, Halogen bonding at the active sites of human cathepsin L and MEK1 kinase: efficient interactions in different environments, ChemMedChem, 6 (2011) 2048-2054.
[49] R. Wilcken, M.O. Zimmermann, A. Lange, A.C. Joerger, F.M. Boeckler, Principles and Applications of Halogen Bonding in Medicinal Chemistry and Chemical Biology, J Med Chem, (2013).
[50] W.K. Hagmann, The many roles for fluorine in medicinal chemistry, J Med Chem, 51 (2008) 4359-4369.
[51] H. Leh, P. Brodin, J. Bischerour, E. Deprez, P. Tauc, J.C. Brochon, E. LeCam, D. Coulaud, C. Auclair, J.F. Mouscadet, Determinants of Mg2+-dependent activities of recombinant human immunodeficiency virus type 1 integrase, Biochemistry, 39 (2000) 9285-9294.

Figure legends

Figure 1. The general structure of the methylenebisphosphonates under study (**A**) and structures of the compounds synthesized (**B**). First prepared compounds are in italic

Figure 2. ^{31}P NMR spectra of compounds **2a** and **2c**. (A) The pH dependence of the chemical shifts of phosphorus atoms. (B) The variations of the phosphorus atom resonances at various pH in the presence of Mg^{2+} ions. The sample contained both BP at a ratio of 1:2 and Mg^{2+} at a molar concentration twice as high as that of both BPs.

Figure 3. The dependence of the 3'-processing initial rate vs the DNA substrate concentration at varied inhibitor concentrations on double-reciprocal plots. (**A**) Compound **2a** in the presence of Mg^{2+} ions; (**B**) Compound **2c** in the presence of Mg^{2+} ions; (**C**) Compound **2a** in the presence of Mn^{2+} ions; (**D**) Compound **2c** in the presence of Mn^{2+} ions.

Figure 4. Binding of the DNA substrate to IN alone and IN-LEDGF complex. **A**. The dependency of the binding efficacy vs IN concentration ($[IN_{eq}]$=[IN] for IN and $[IN_{eq}]$ = 4*[IN/LEDGF] for the complex) **B**. The kinetics of the DNA substrate binding to IN alone and to the IN-LEDGF complex (IN_{eq} = 100 nM). The binding kinetics at initial time points are shown at the insert.

Table 1. Inhibition of the DNA-binding and catalytic activities of HIV-1 IN by BPs in the presence of different metal cofactors.

Compound	Inhibitory effect of the tested BPs, IC_{50} (μM)							
	IN activity						Activity of the IN-LEDGF complex in 3'-processing	
	Binding		3'-processing		ST			
	Mg^{2+}	Mn^{2+}	Mg^{2+}	Mn^{2+}	Mg^{2+}	Mn^{2+}	Mg^{2+}	Mn^{2+}
	1	**2**	**3**	**4**	**5**	**6**	**7**	**8**
2a	150	>500	35	5	45	4	>250	4.5
2b	70	>500	20	5	42	6	>250	8
2c	>256	>500	7	2	3	2	7	2
2d	130	>500	30	5	30	5	>250	6
5	100	>500	20	0.8	16	0.8	nd*	nd

* - not determined

Figure 1

A

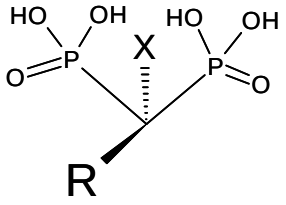

B

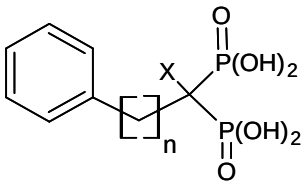

1a, n=1, X=OH
1b, n=2, X=OH
1c, n=4, X=OH
1d, n=1, X=NH_2

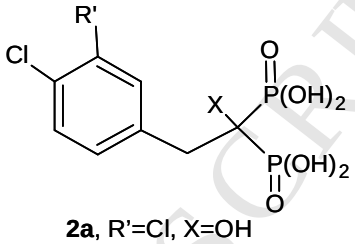

2a, R'=Cl, X=OH
2b, R'=H, X=OH
2c, R'=Cl, X=NH_2
2d, R'=Cl, X=H

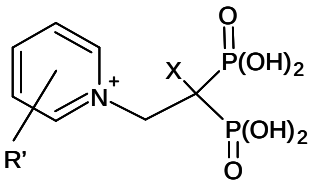

3a, R'=H, X=OH
***3b**, R'=H, X=NH_2*
3c, R'=p-Ph, X=OH
3d, R'=m-OH, X=OH
***3e**, R'=o-Et, X=OH*

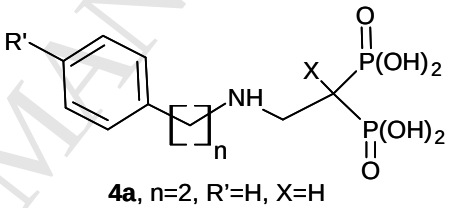

4a, n=2, R'=H, X=H
4b, n=0, R'=H, X=H
***4c**, n=0, R'=I, X=H*

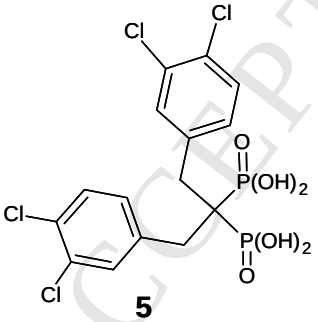

5

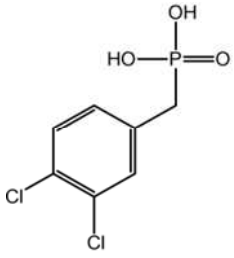

6

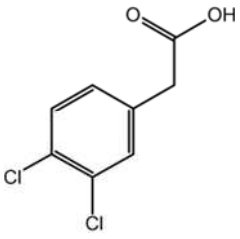

7

Figure 2.

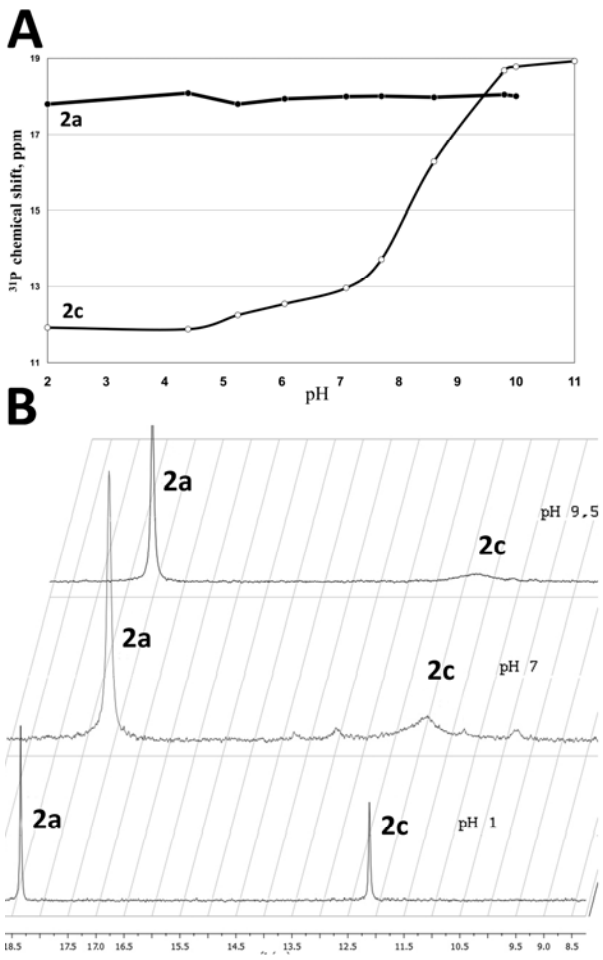

Figure 3

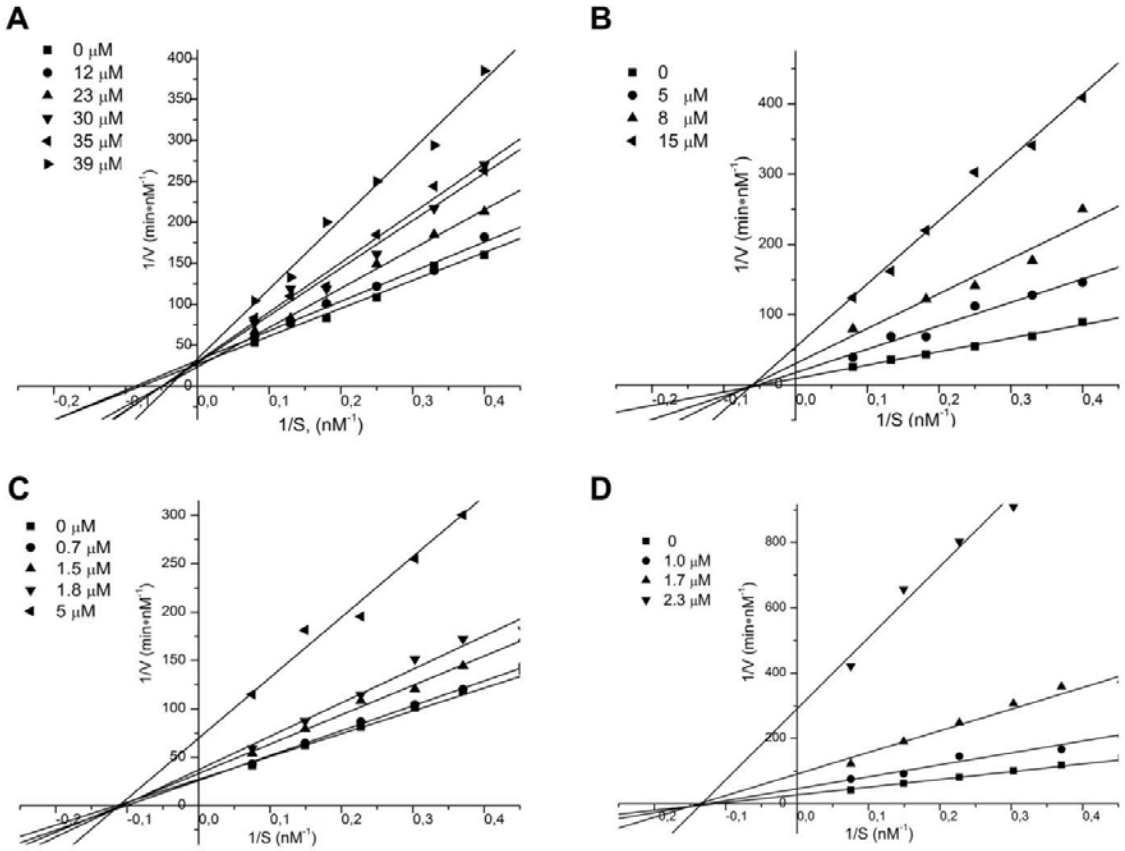

Figure 4

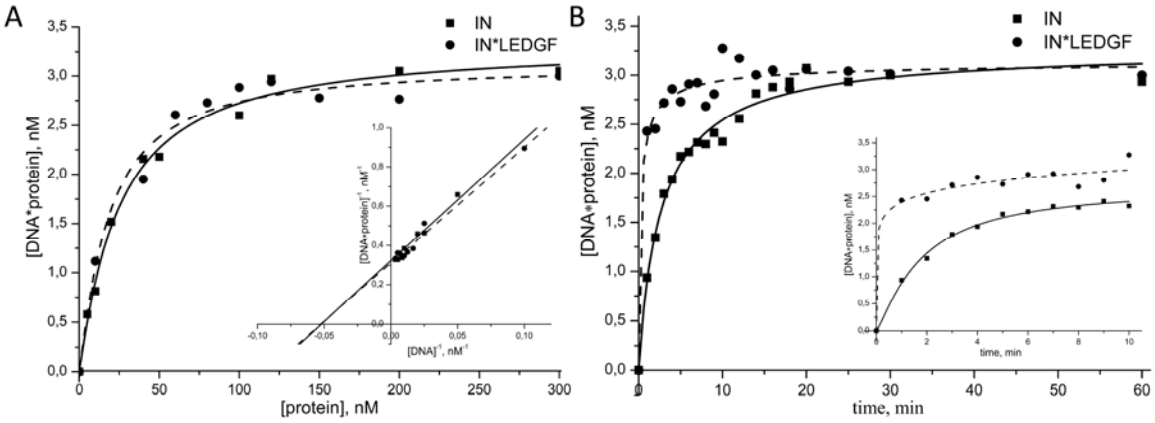

Method A.

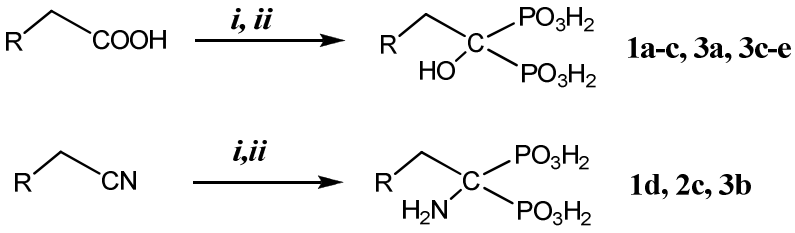

i- $H_3PO_3/POCl_3$, CH_3SO_3H, 75-80°C *ii*- 3 M HCl, reflux

Method B.

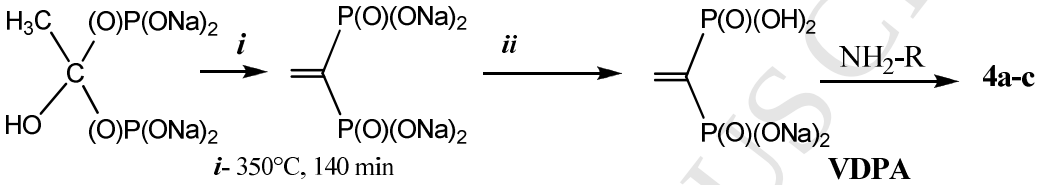

i- 350°C, 140 min
ii- CO_2 gas

Method C.

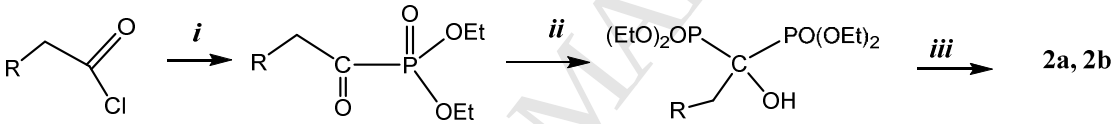

i- $(EtO)_3P$ *ii*- $(EtO)_2P(OH)$, iPr_2NH *iii*- TMSBr then MeOH

Method D.

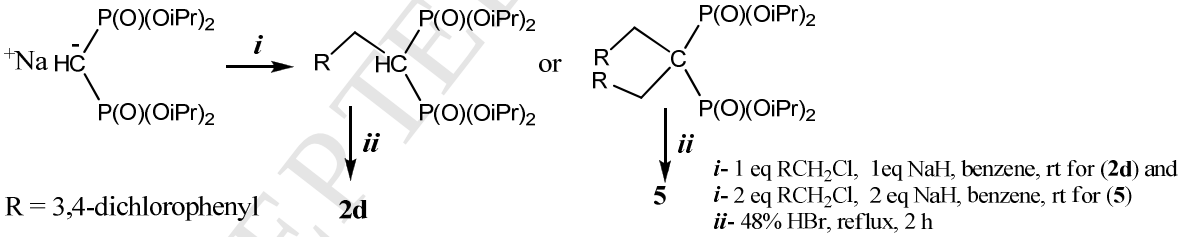

R = 3,4-dichlorophenyl **2d**

i- 1 eq RCH_2Cl, 1eq NaH, benzene, rt for (**2d**) and
i- 2 eq RCH_2Cl, 2 eq NaH, benzene, rt for (**5**)
ii- 48% HBr, reflux, 2 h

Supporting Information

Specific features of HIV-1 integrase inhibition by bisphosphonate derivatives

Julia Agapkina[†,||], Dmitry Yanvarev[*,‡,||], Andrey Anisenko[†], Sergey Korolev[†], Jouko Vepsäläinen[§], Sergey Kochetkov[‡,†], Marina Gottikh[†]

[†]*-Lomonosov Moscow State University, Chemistry Department and Belozersky Institute of Physical and Chemical Biology, Moscow, Russia;* [‡]*-Engelhardt Institute of Molecular Biology, Russian Academy of Sciences, Moscow, Russia;* [§] *-School of Pharmacy, Biocenter Kuopio, University of Eastern Finland, Kuopio, Finland.*

|| these authors contributed equally to this work

***corresponding author**: Dmitry V. Yanvarev. E-mail: JDmitry@hotmail.com, tel.+7(926)7025449

Table of contents:

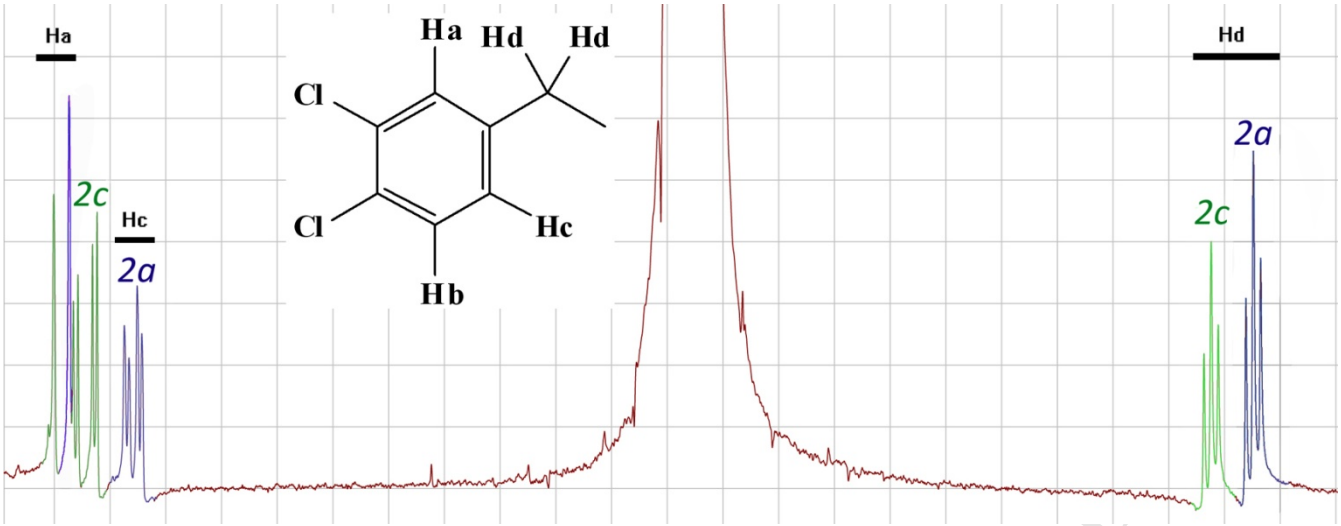

Figure S1. ^{1}H NMR chemical shifts of selected protons. The effect of the X substituent on the electron density at nuclei H for compounds **2a** and **2c**. The electron density reduces from upfield to downfield.

Synthetic procedures.

Pyridinium acetic acids and pyridinium acetonitriles.

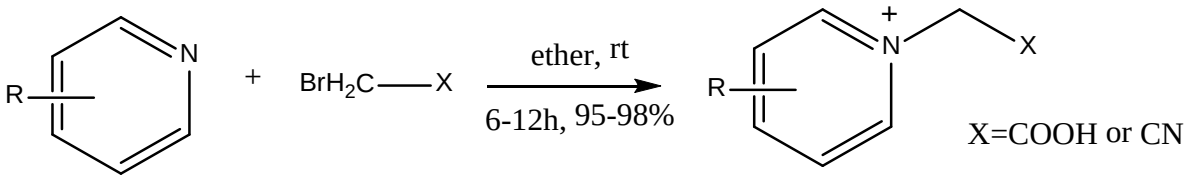

Bromoacetic acid or bromoacetonitrile (6 mmol) was added to a solution of the pyridine derivative (5 mmol) in ether (15 mL) and the reaction mixture refluxed for 6-8 h to give the substituted pyridinium bromides as white precipitates. The precipitates were filtered, washed with ether (2x10 mL) and dried in vacuum. Yields were >95%.

Vinylidenediphosphonic acid (VDPA).

VDPA was prepared by thermal dehydration of tetrasodium salt of etidronic acid followed by partial deionization of tetrasodium VDPA by CO_2 gas. The thermal conditions and dehydration time were optimized (350°C, 5 h) to get 97-100% conversion of etidronate. Reaction was monitored by ^{31}P NMR analysis, which revealed VDPA and PP_i to be the main reaction products (>90%).

Muffle furnace dried (250°C, 2 h) tetrasodium etidronate was heated 5 h at 350°C. After the reaction was completed and cooled to room temperature, the residue was dissolved in a minimal amount of water at 20°C, and insoluble materials were filtered off. The filtrate was diluted two-fold with water and a CO_2 flow was passed through at +5°C up to pH 6. The solution was left at this temperature for additional 5-6 h and the precipitated $NaHCO_3$ was filtered off. Since we failed to crystallize VDPA either from water/alcohols or from water/acetone solutions, we used it as a water solution with concentration measured by ^{1}H-NMR.

kr7132

BPH-1a

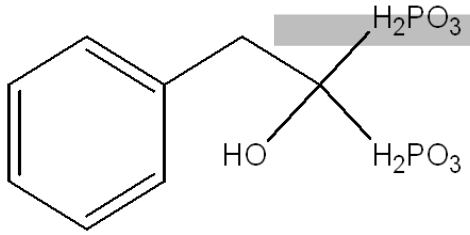

^{1}H NMR (400 MHz, D_2O) δ 3.32 (t, J = 13.7 Hz, 2H).

A (t)
3.32

7.38
7.37
7.30
7.28
3.35
3.32
3.28
1.19
1.19

5.15
2.00

tBu-OD

7.5 7.0 6.5 6.0 5.5 5.0 4.5 4.0 3.5 3.0 2.5 2.0 1.5
f1 (мд)

BPH-1
D2O pH =1

31P

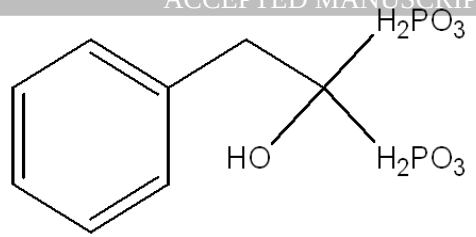

BPH-1a

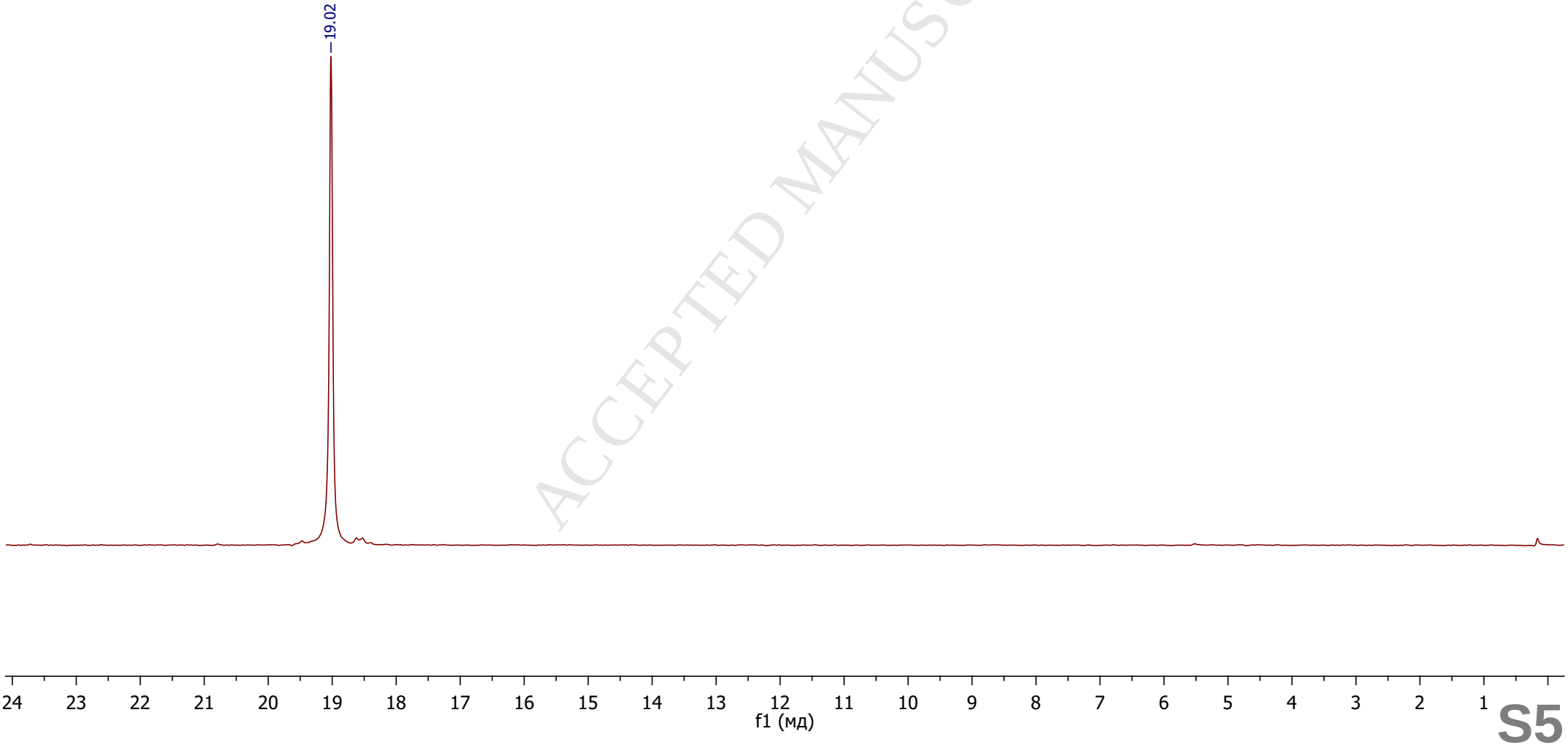

kr7158

1H

BPH-1c

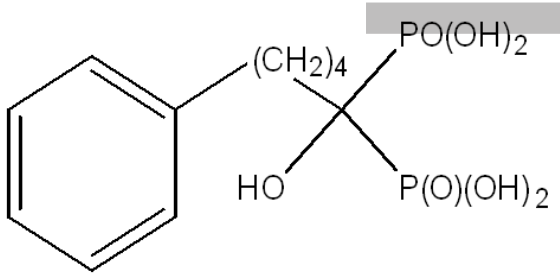

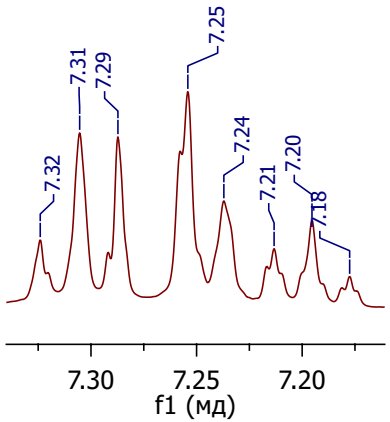

kr7158c13dec

13C

BPH-1c

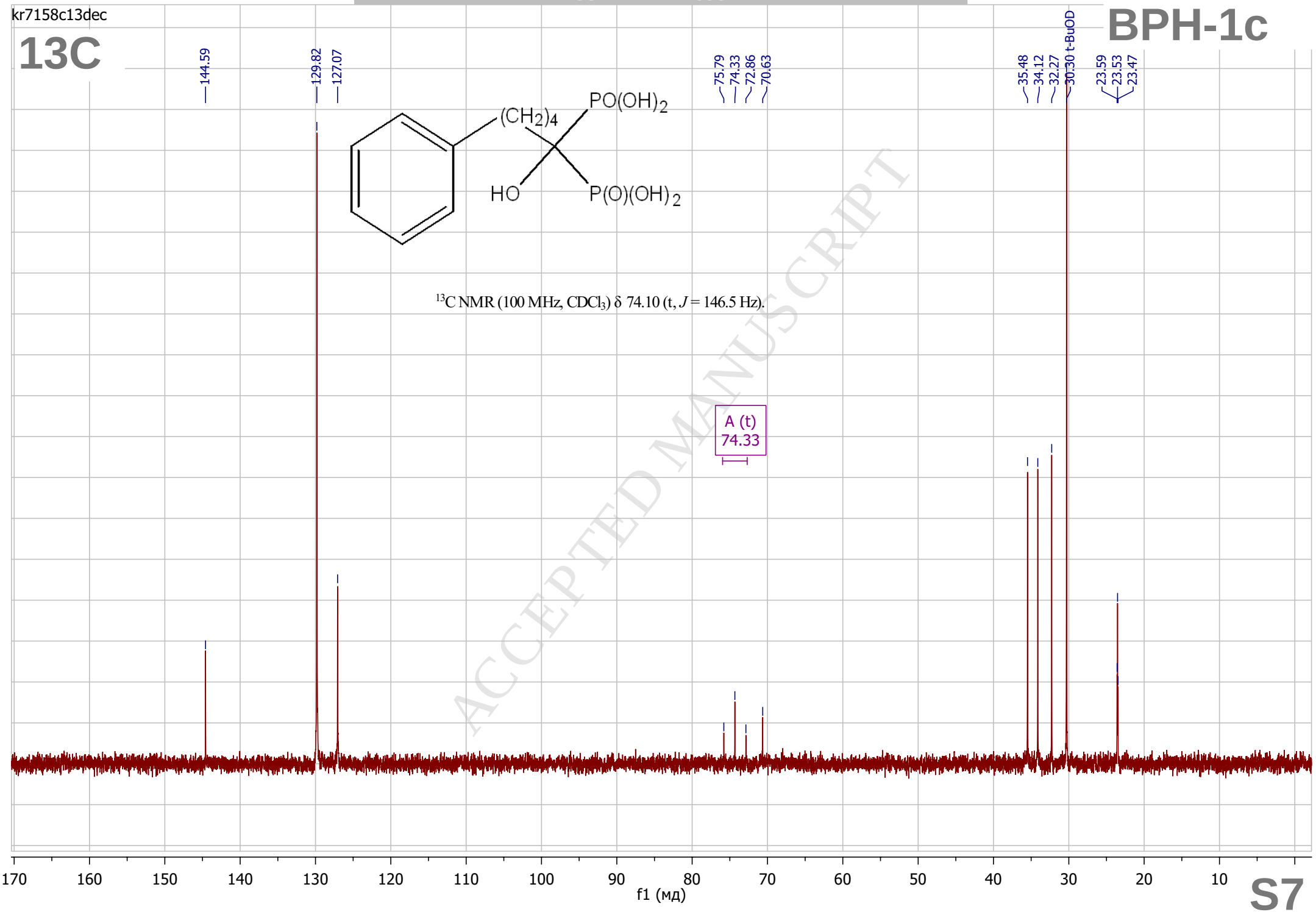

^{13}C NMR (100 MHz, $CDCl_3$) δ 74.10 (t, J = 146.5 Hz).

kr7158p31sup

31P

BPH-1c

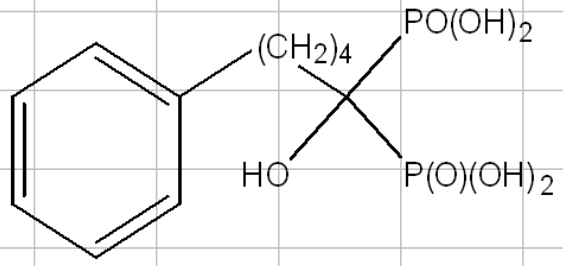

18.53

65 60 55 50 45 40 35 30 25 20 15 10 5 0 -5 -10 -15

f1 (мд)

kr7816

1H

BPH-1d

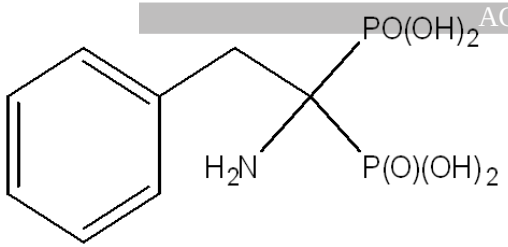

^{1}H NMR (400 MHz, D_2O) δ 3.42 (t, J = 12.5 Hz, 2H).

kr7870c13dec

13C

BPH-1d

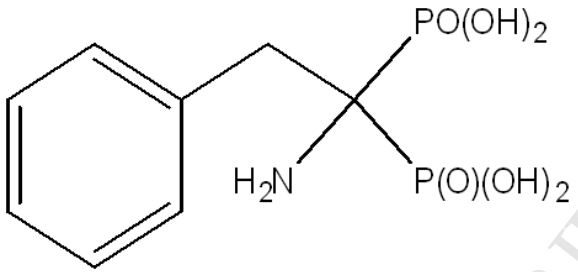

^{13}C NMR (100 MHz, D_2O) δ 58.46 (t, J = 129.4 Hz).

kr7825p31nd

BPH-1d

31P

^{31}P NMR (161 MHz, D_2O) δ 12.42 (t, J = 12.1 Hz).

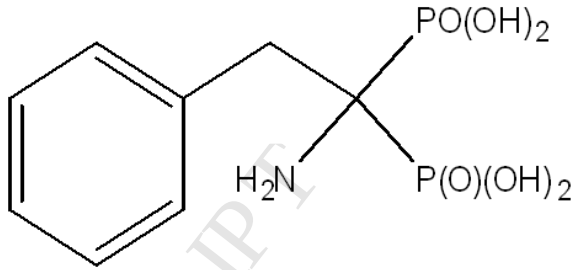

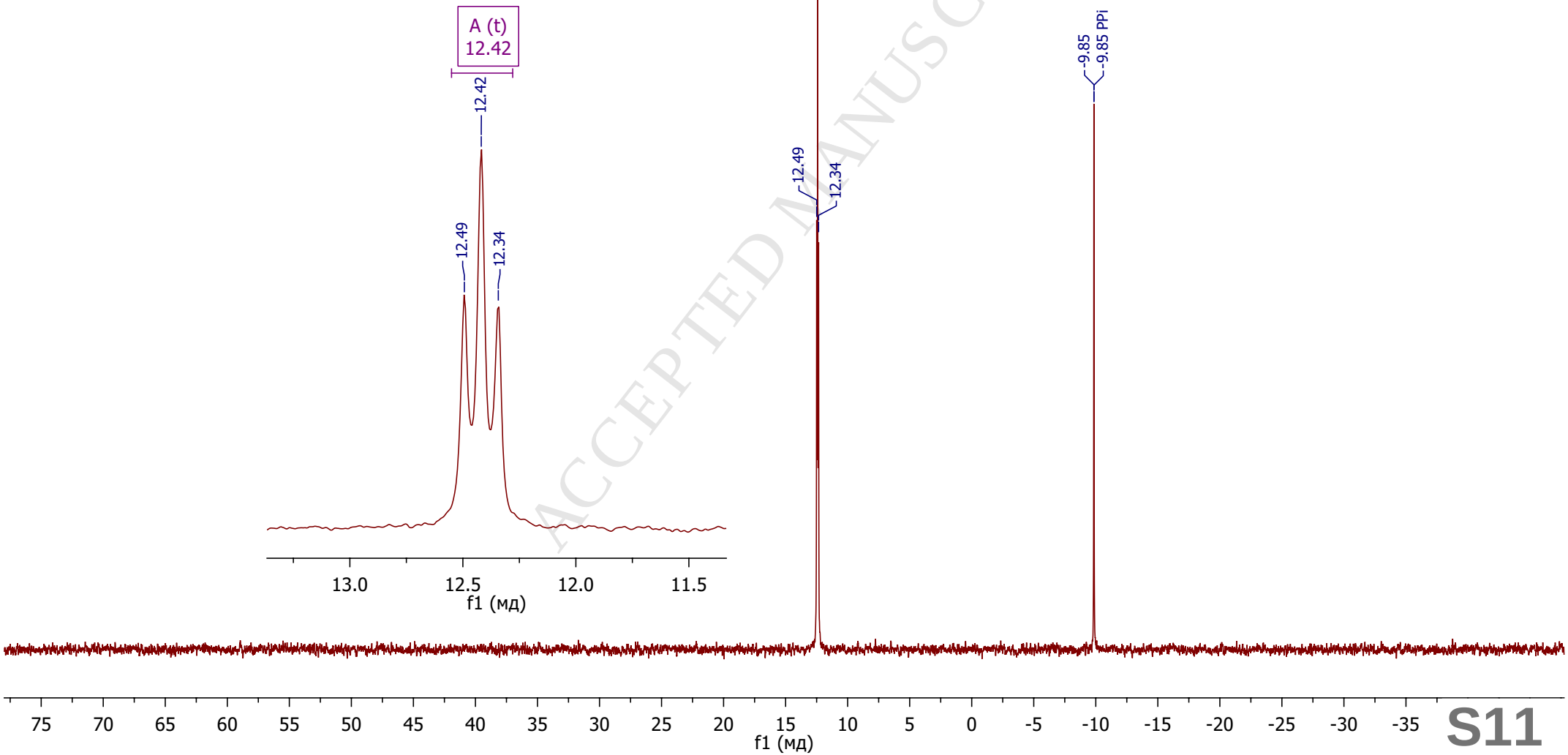

kr7144

1H

BPH-2a

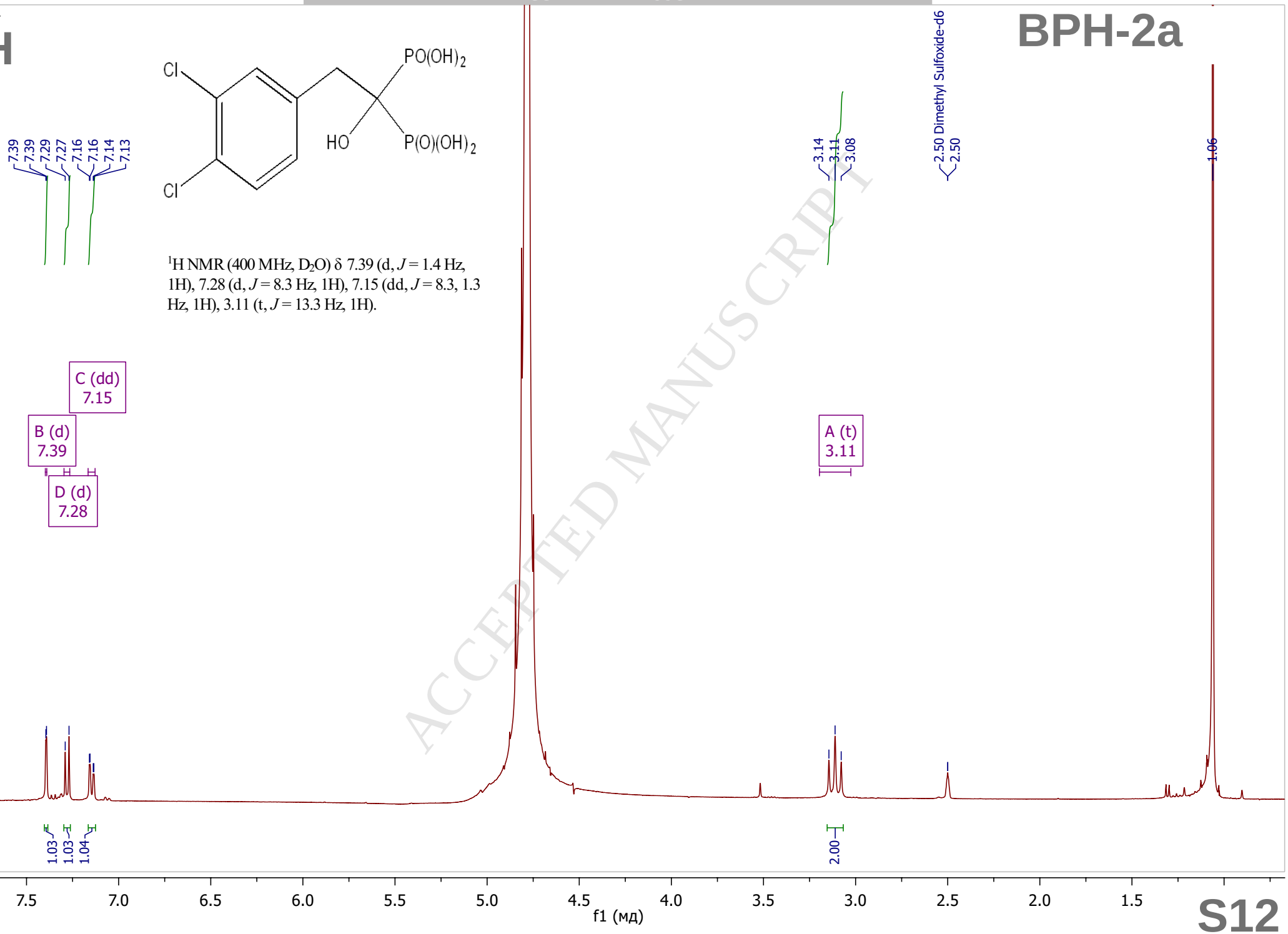

^{1}H NMR (400 MHz, D_2O) δ 7.39 (d, J = 1.4 Hz, 1H), 7.28 (d, J = 8.3 Hz, 1H), 7.15 (dd, J = 8.3, 1.3 Hz, 1H), 3.11 (t, J = 13.3 Hz, 1H).

kr7144c13dec

13C

BPH-2a

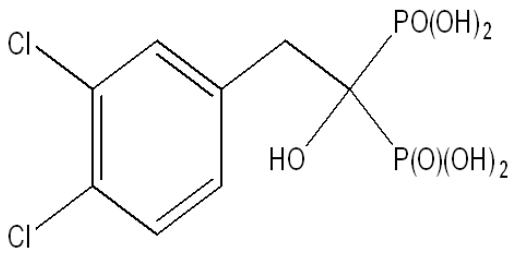

^{13}C NMR (100 MHz, D2O+25% DMSO-d6) δ 74.32 (t, *J* = 147.2 Hz).

kr8059p31sup

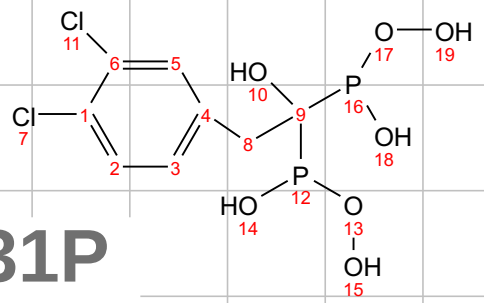

31P

BPH-2a

17.84

3.30

1.10

98.33

0.89

0.78

36 34 32 30 28 26 24 22 20 18 16 14 12 10 8 6 4 2 0 -2

f1 (мд)

kr8181

BPH-2c

1H

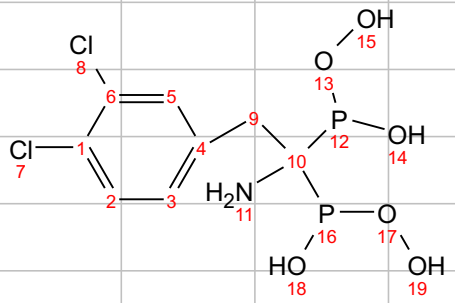

tBuOD

^{1}H NMR (400 MHz, D_2O) δ 7.55 (d, J = 2.0 Hz, 1H), 7.39 (d, J = 8.2 Hz, 1H), 7.30 (dd, J = 8.3, 2.0 Hz, 1H), 3.16 (t, J = 12.0 Hz, 2H).

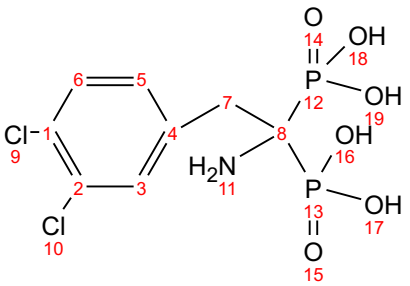

^{13}C NMR (101 MHz, D_2O) δ 57.47 (t, J = 123.6 Hz).

31P

BPH-2c

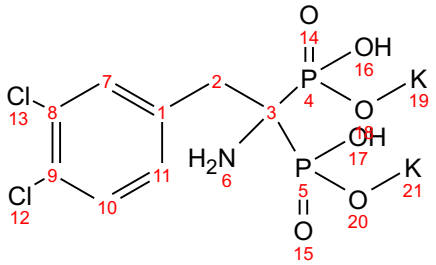

kr8748

BPH-2d

1H

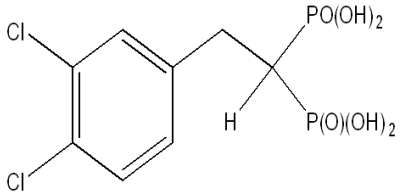

^{1}H NMR (400 MHz, D_2O) δ 7.39 (d, J = 8.3 Hz, 1H), 7.26 (d, J = 7.2 Hz, 1H).

^{1}H NMR (400 MHz, D_2O) δ 2.09 (ddd, J = 21.2, 13.9, 6.7 Hz, 1H).

^{1}H NMR (400 MHz, D_2O) δ 3.03 (td, J = 15.3, 6.8 Hz, 1H).

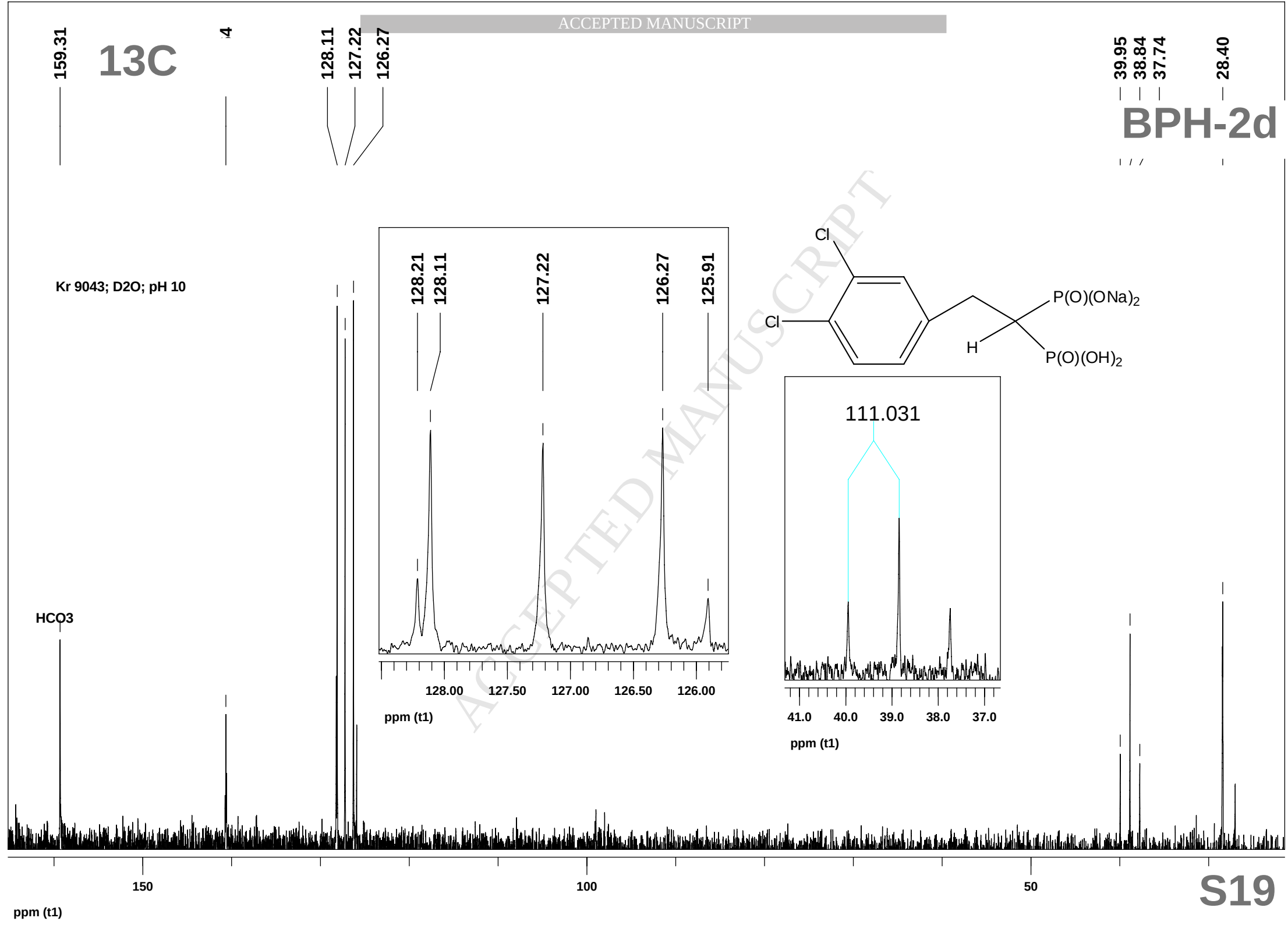

Kr 8748; D2O; pH 10

BPH-2d

31P

19.43

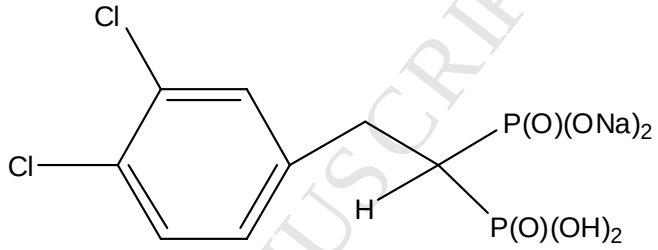

35.0 30.0 25.0 20.0 15.0 10.0 5.0 0.0

ppm (t1)

BPH-3a

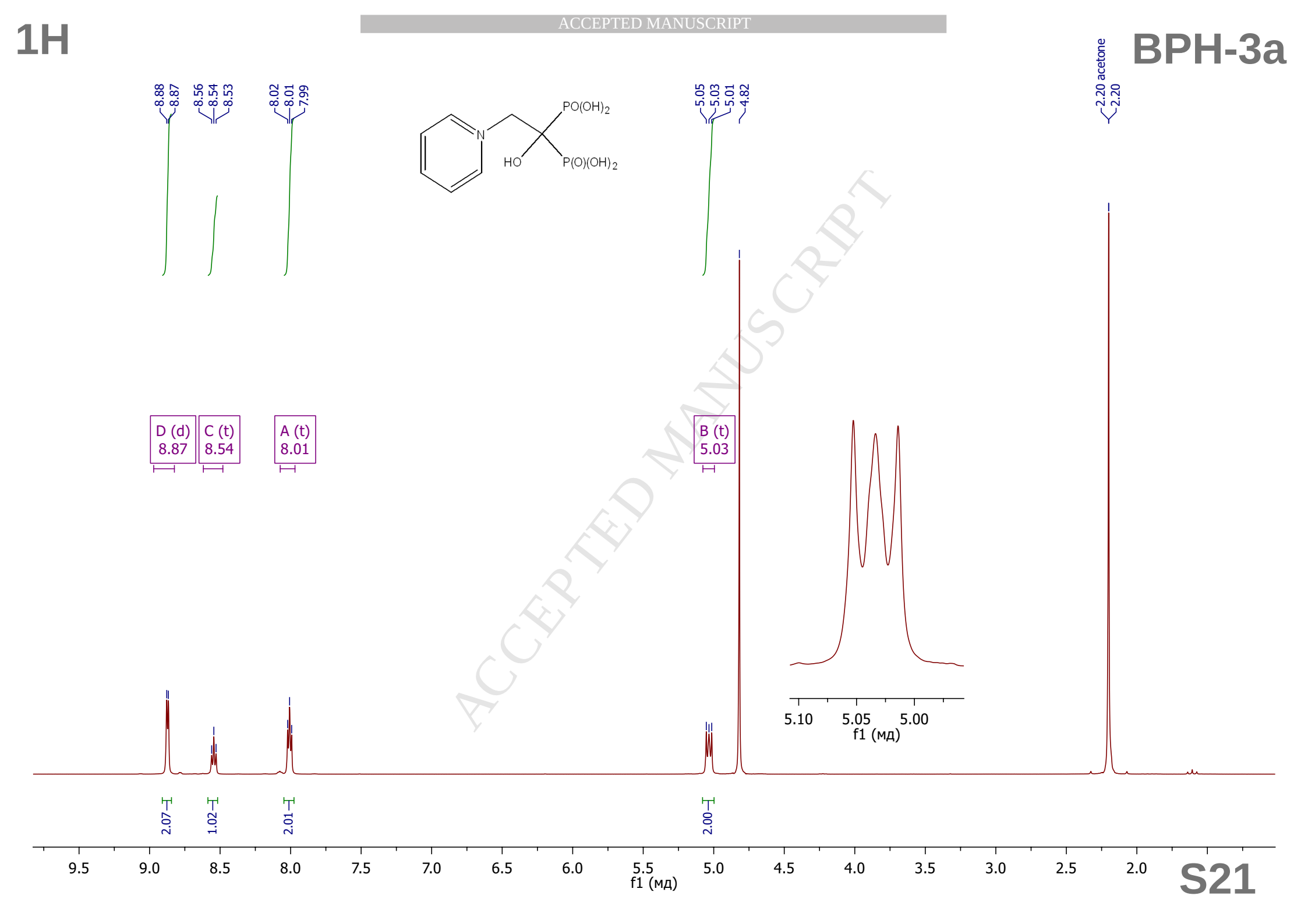

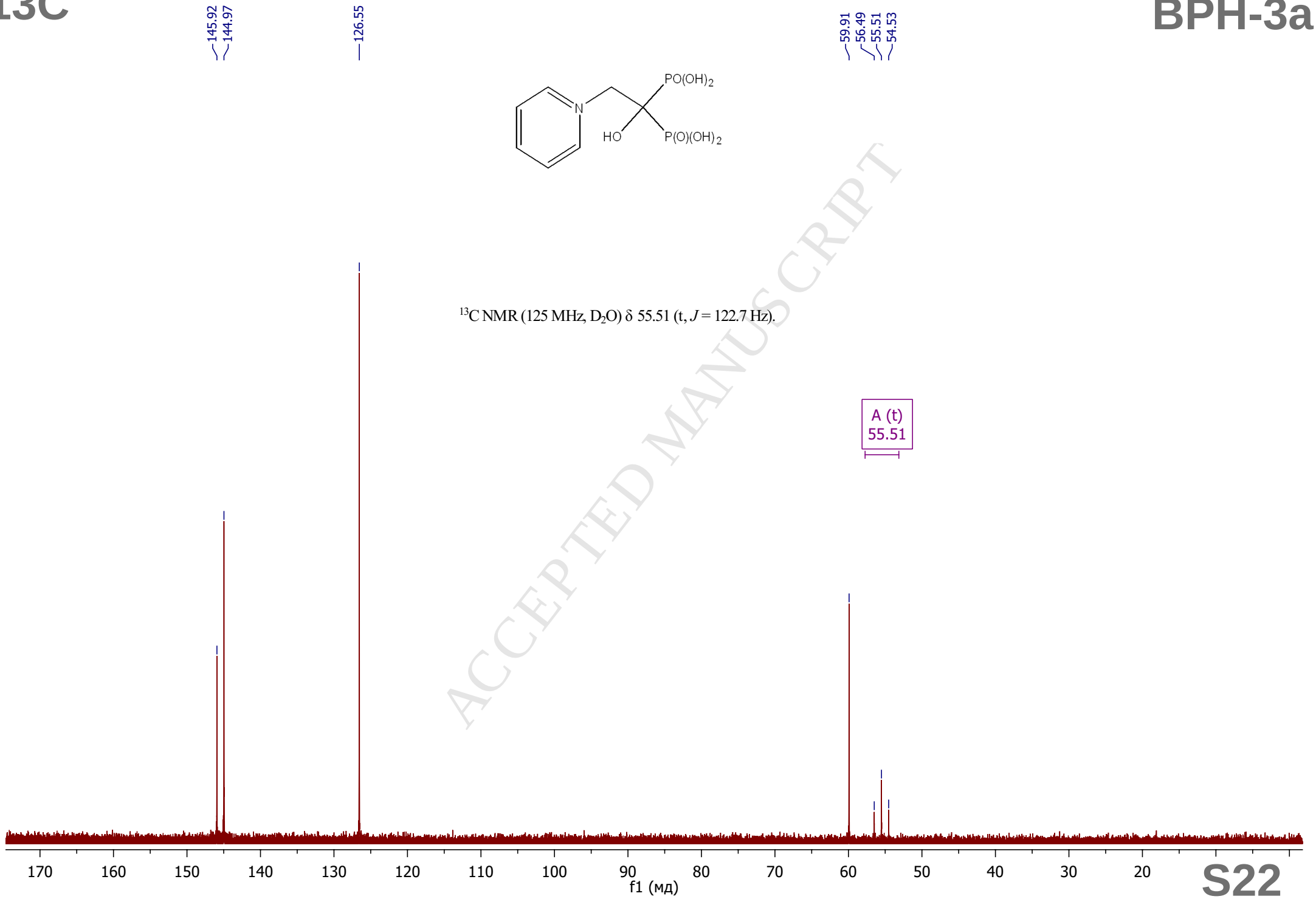

^{13}C NMR (125 MHz, D_2O) δ 55.51 (t, J = 122.7 Hz).

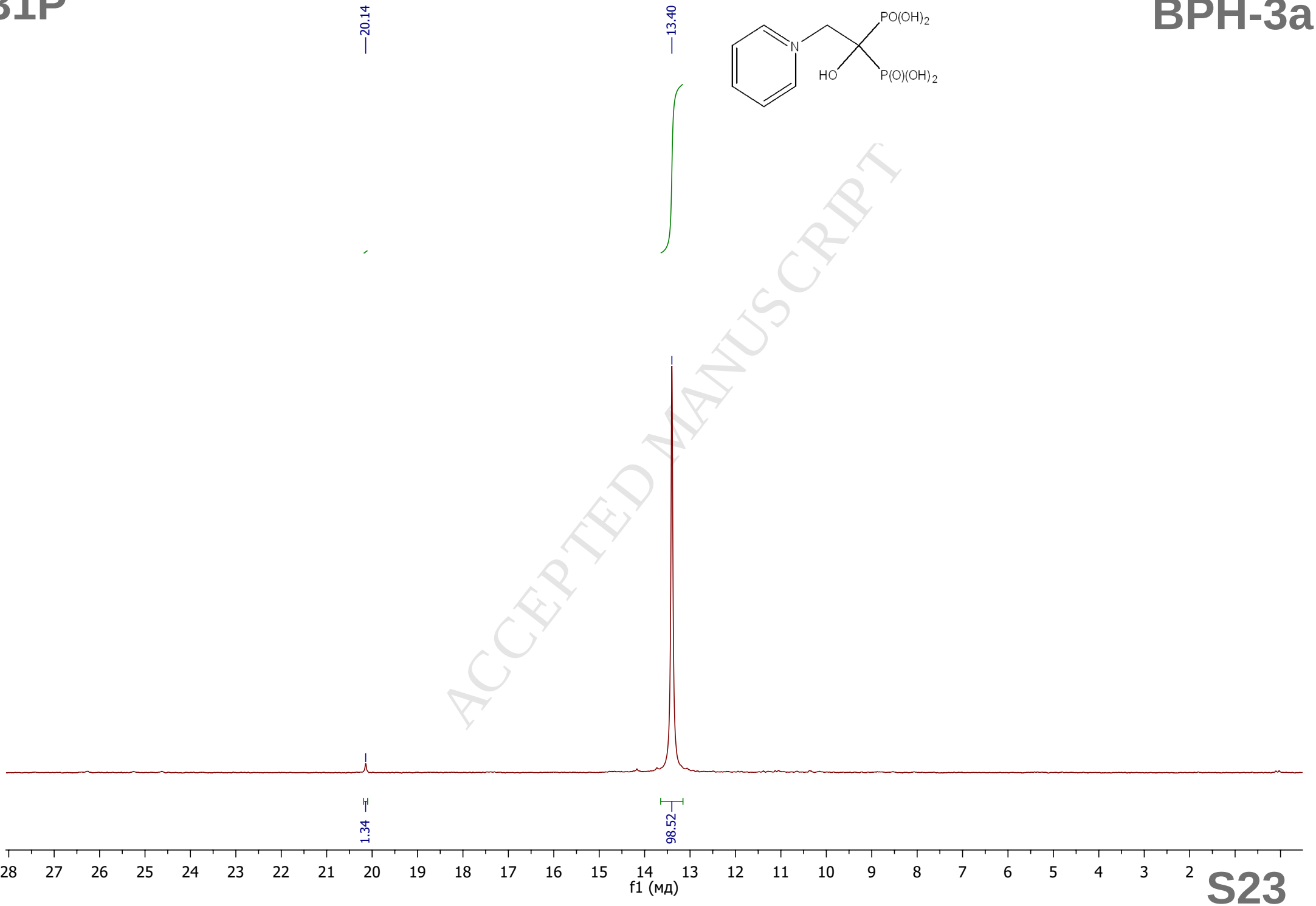

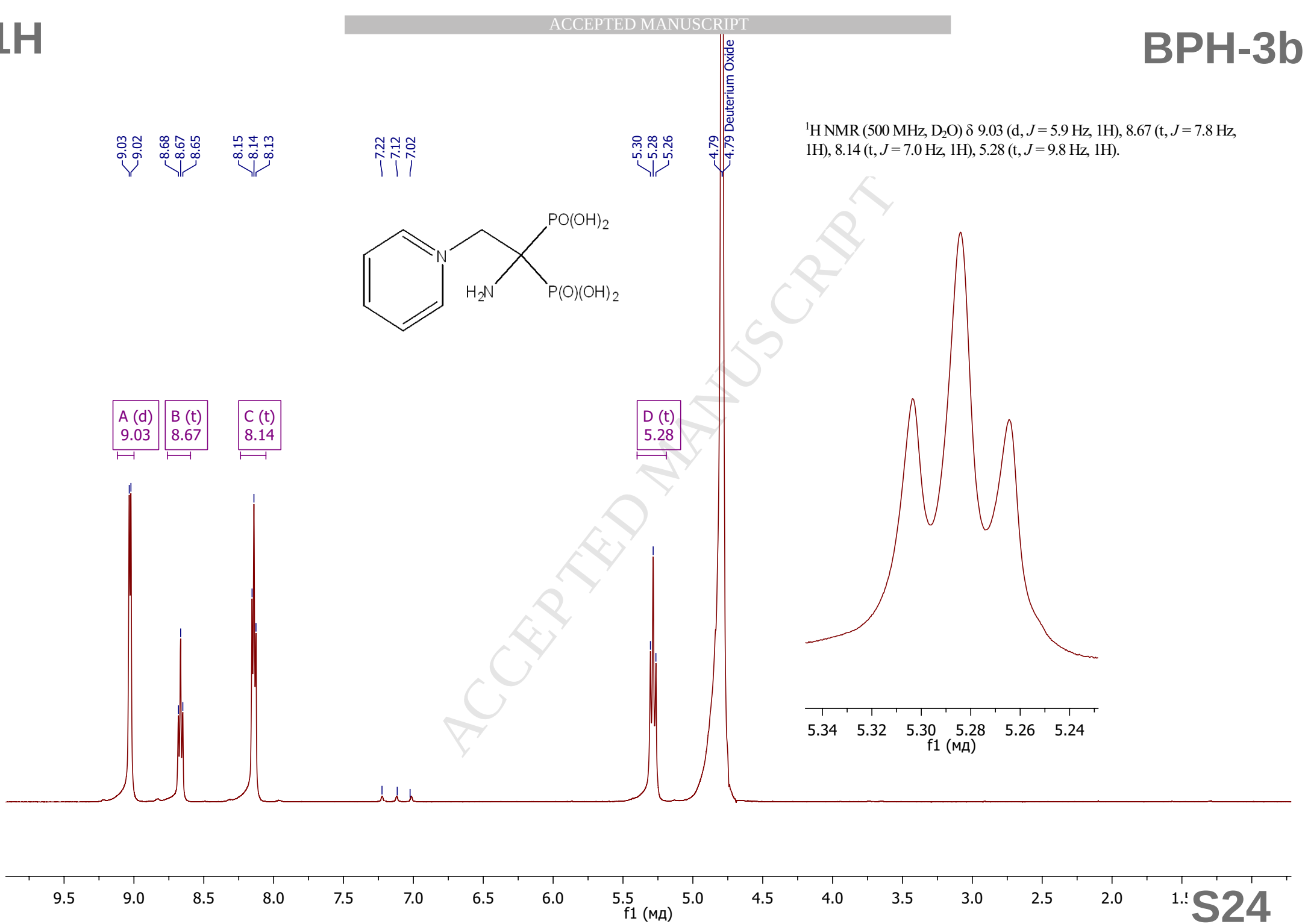

^{1}H NMR (500 MHz, D_2O) δ 9.03 (d, J = 5.9 Hz, 1H), 8.67 (t, J = 7.8 Hz, 1H), 8.14 (t, J = 7.0 Hz, 1H), 5.28 (t, J = 9.8 Hz, 1H).

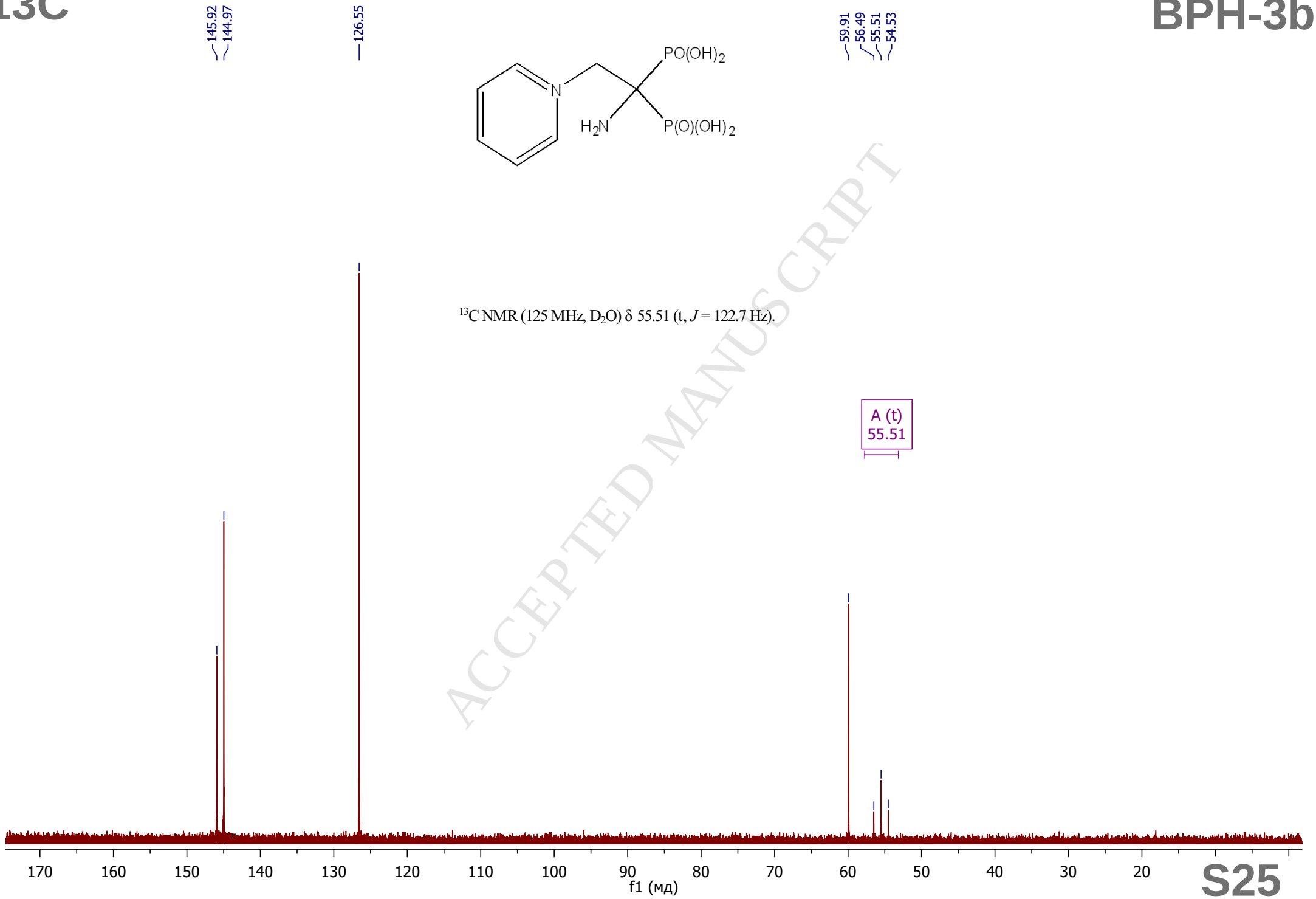

^{13}C NMR (125 MHz, D_2O) δ 55.51 (t, J = 122.7 Hz).

31P

BPH-3b

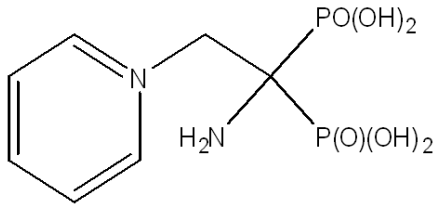

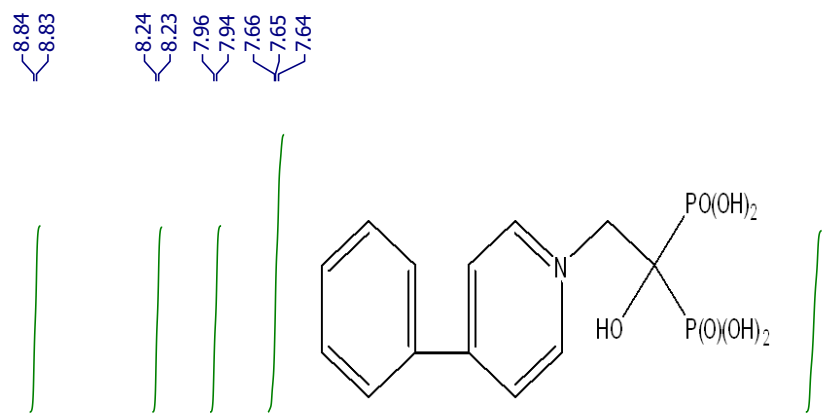

^{1}H NMR (500 MHz, D_2O) δ 8.84 (d, J = 6.7 Hz, 1H), 8.24 (d, J = 6.8 Hz, 1H), 7.95 (d, J = 6.7 Hz, 1H), 5.01 (t, J = 9.7 Hz, 2H).

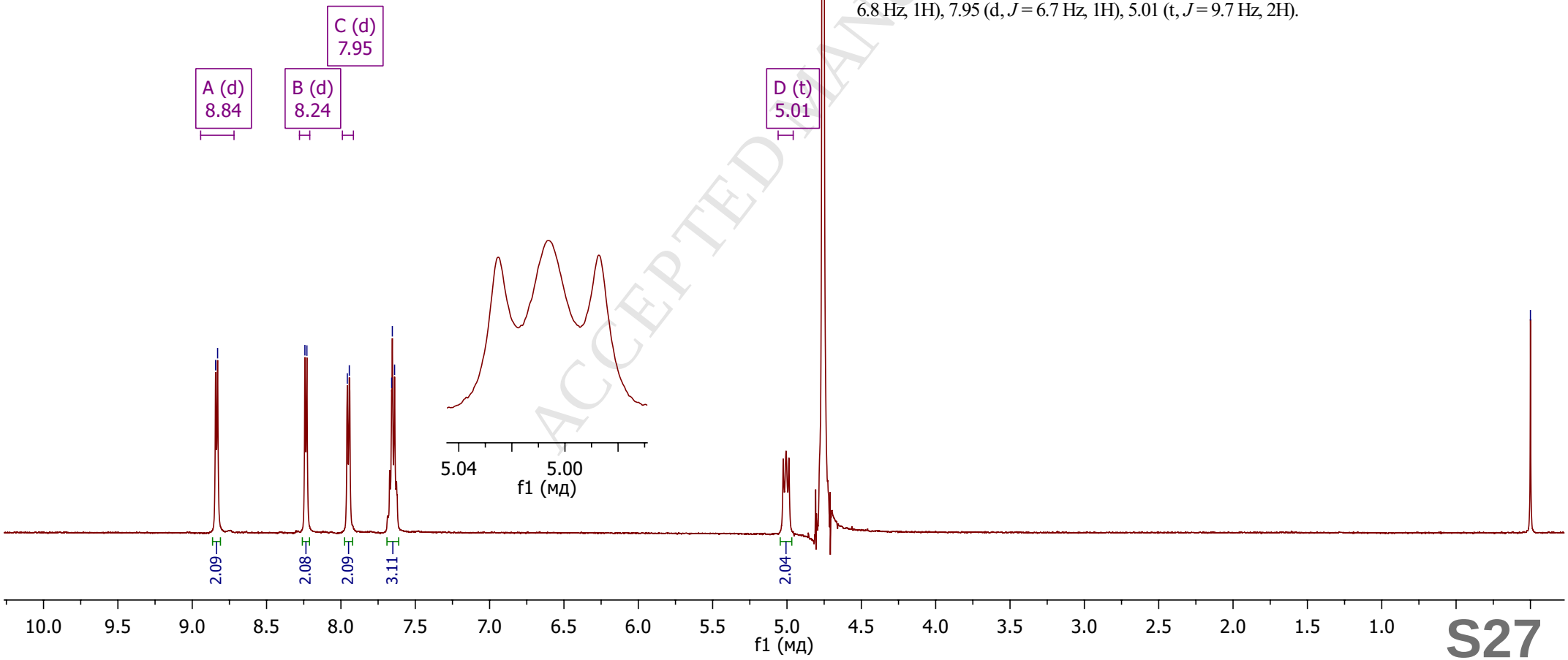

13C

BPH-3c

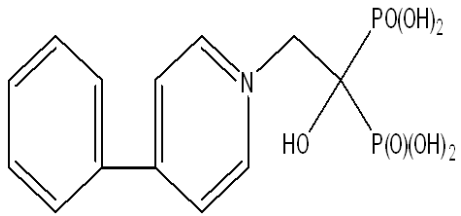

^{13}C NMR (126 MHz, D_2O) δ 76.07 (t, J = 134.2 Hz).

S28

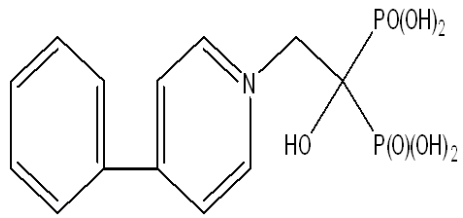

1H

BPH-3d

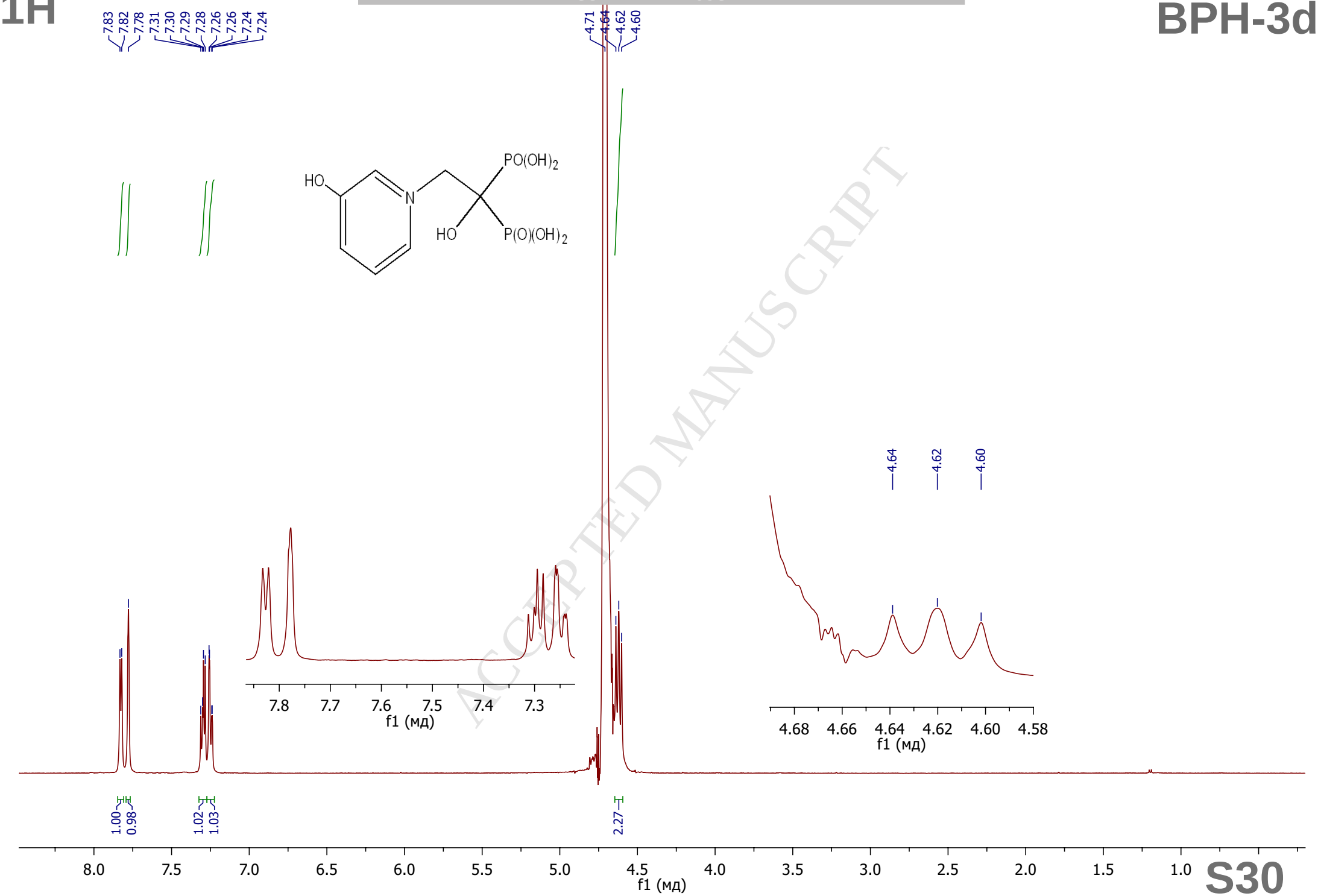

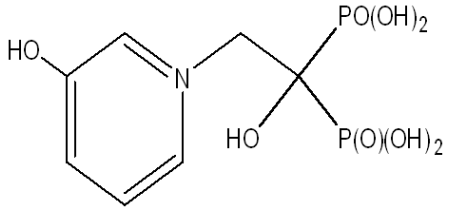

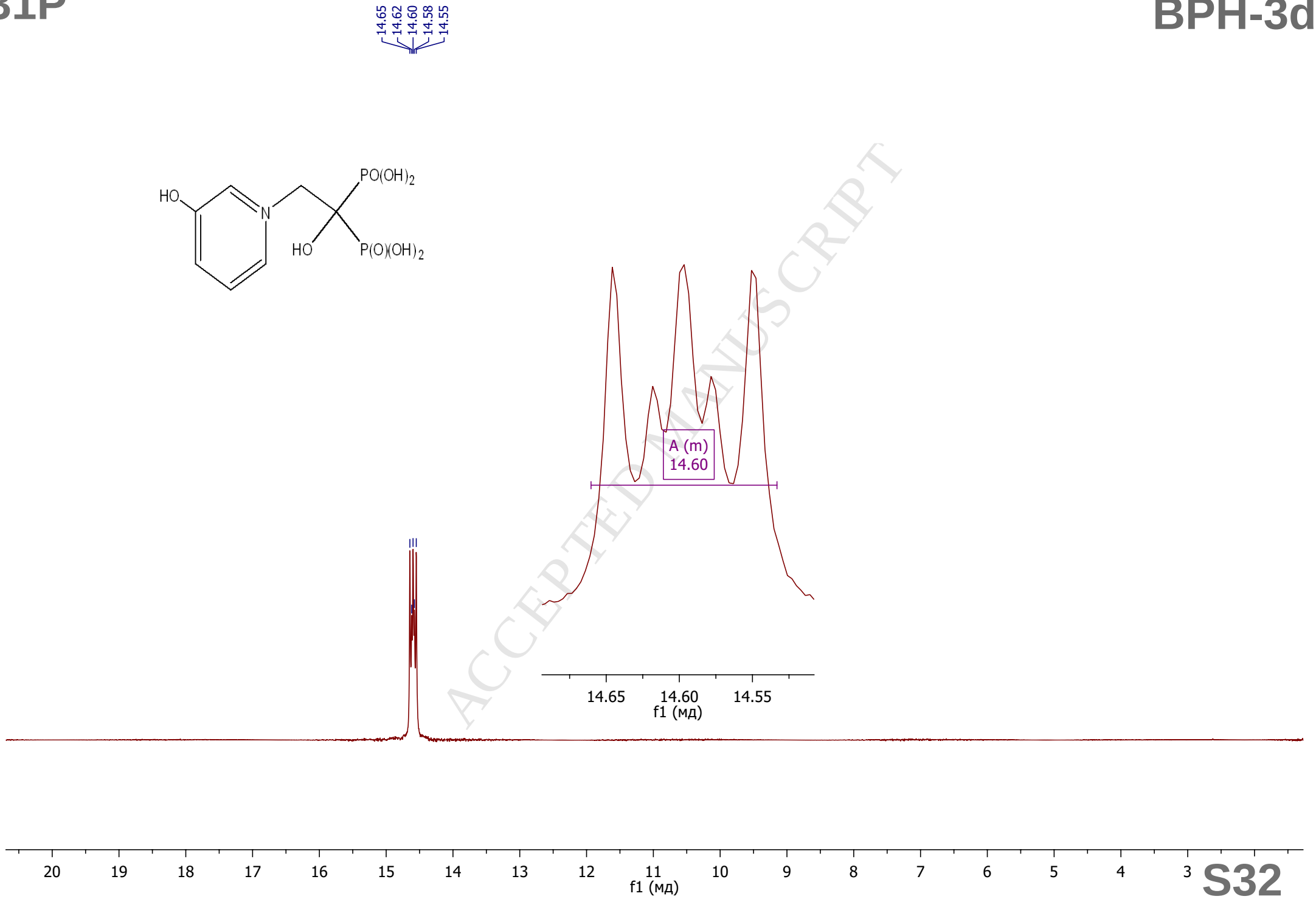

1H

BPH-3e

^{1}H NMR (400 MHz, D_2O) δ 8.82 (d, J = 6.4 Hz, 1H), 8.28 (t, J = 7.9 Hz, 1H), 7.80 (d, J = 8.1 Hz, 1H), 7.67 (t, J = 7.0 Hz, 1H), 4.96 (t, J = 10.1 Hz, 2H), 3.29 (q, J = 7.5 Hz, 2H), 1.27 (t, J = 7.5 Hz, 3H).

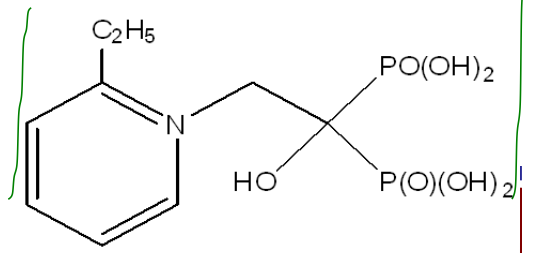

13C

BPH-3e

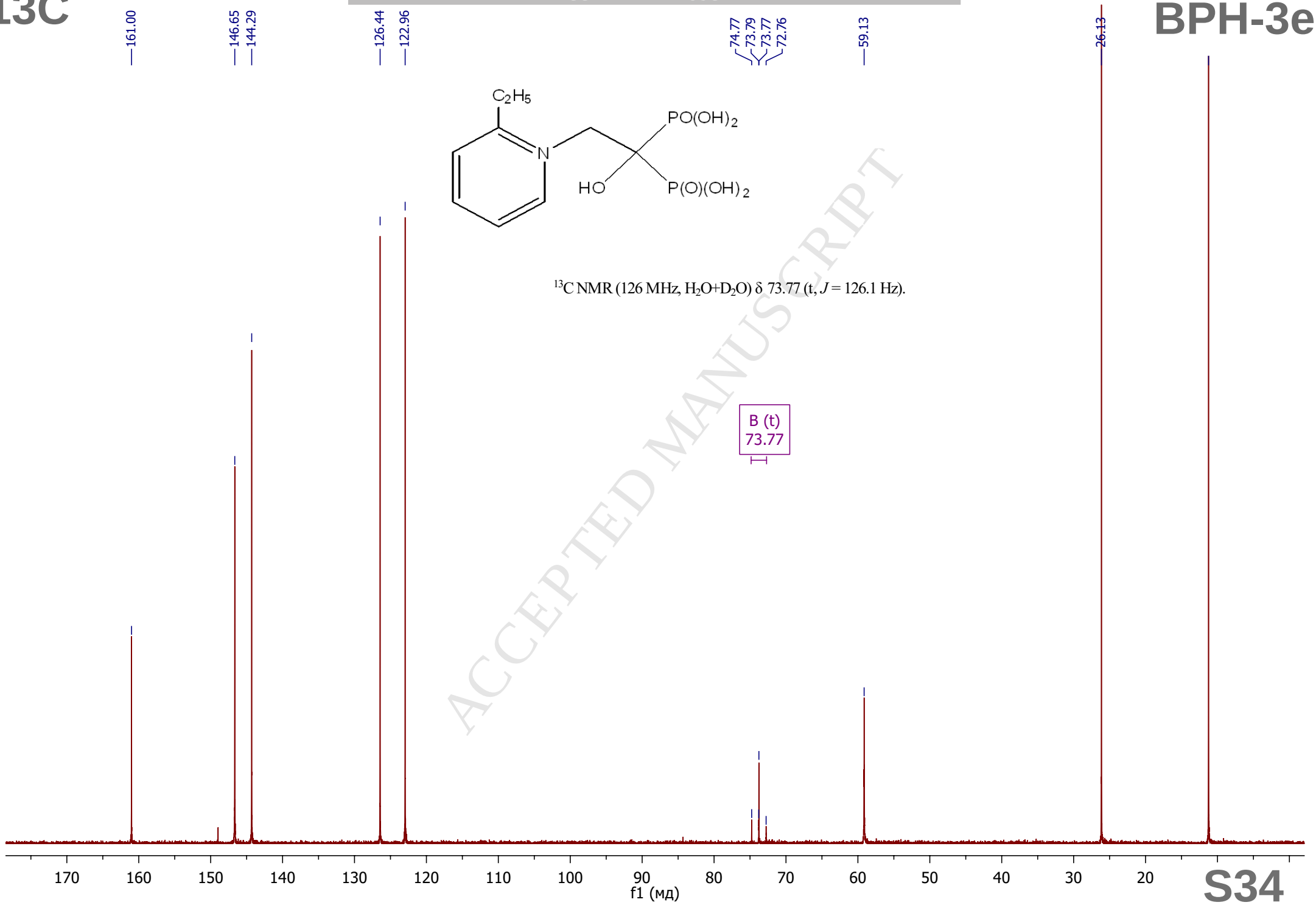

^{13}C NMR (126 MHz, H_2O+D_2O) δ 73.77 (t, J = 126.1 Hz).

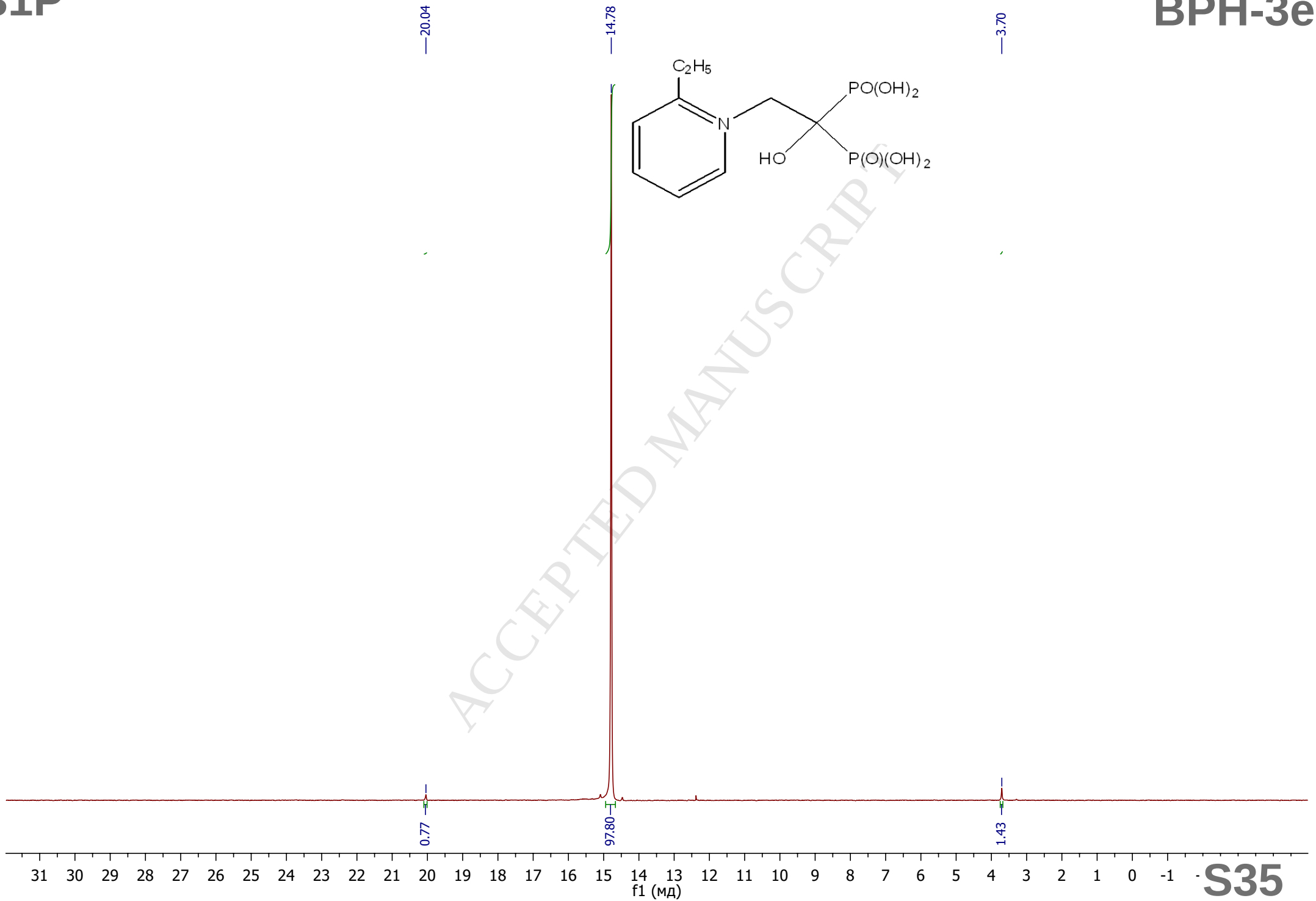

1H

BPH-4a

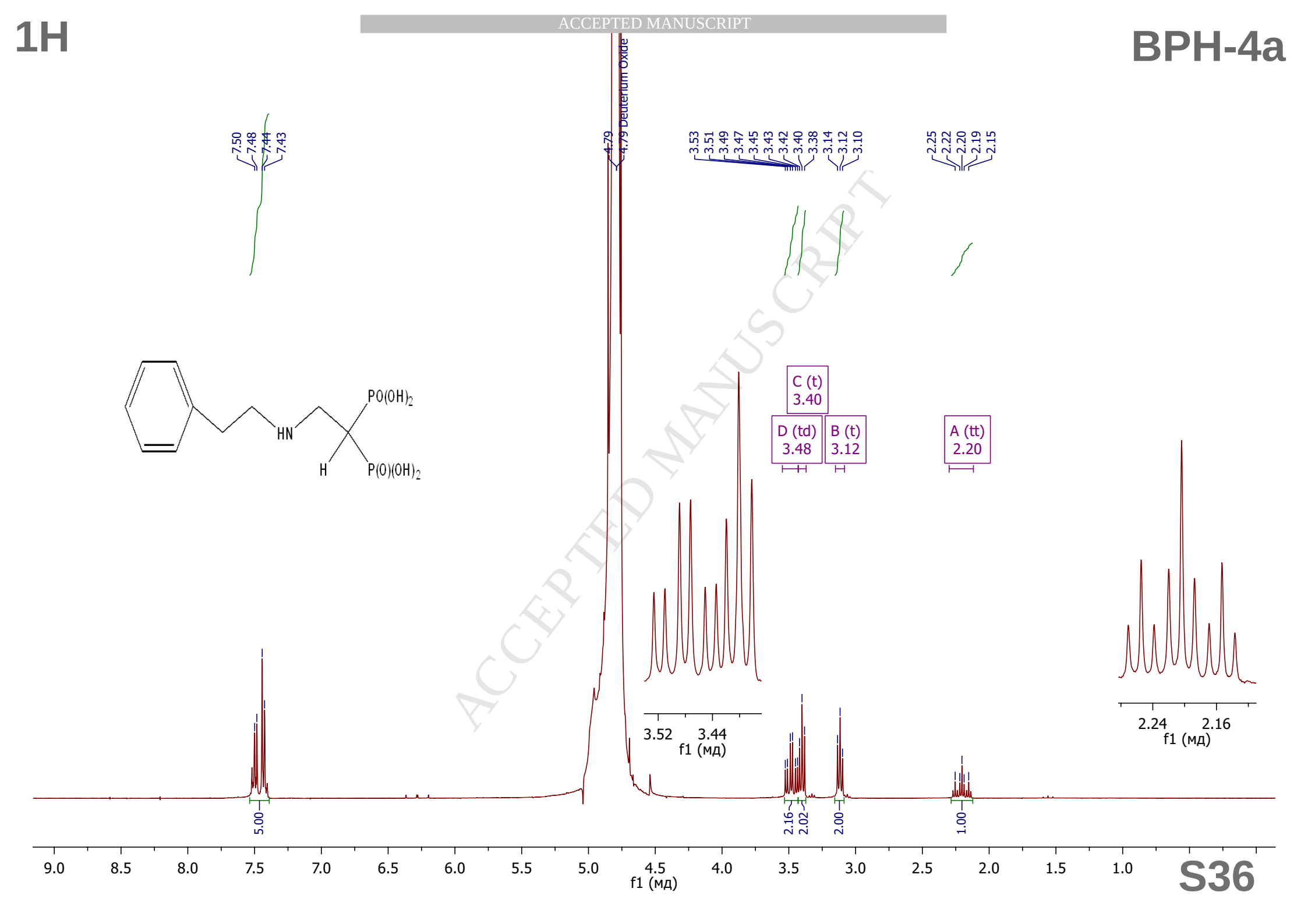

16.20

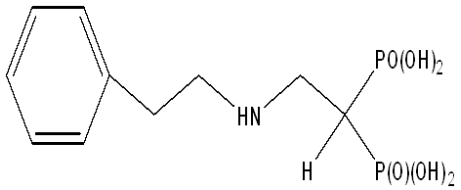

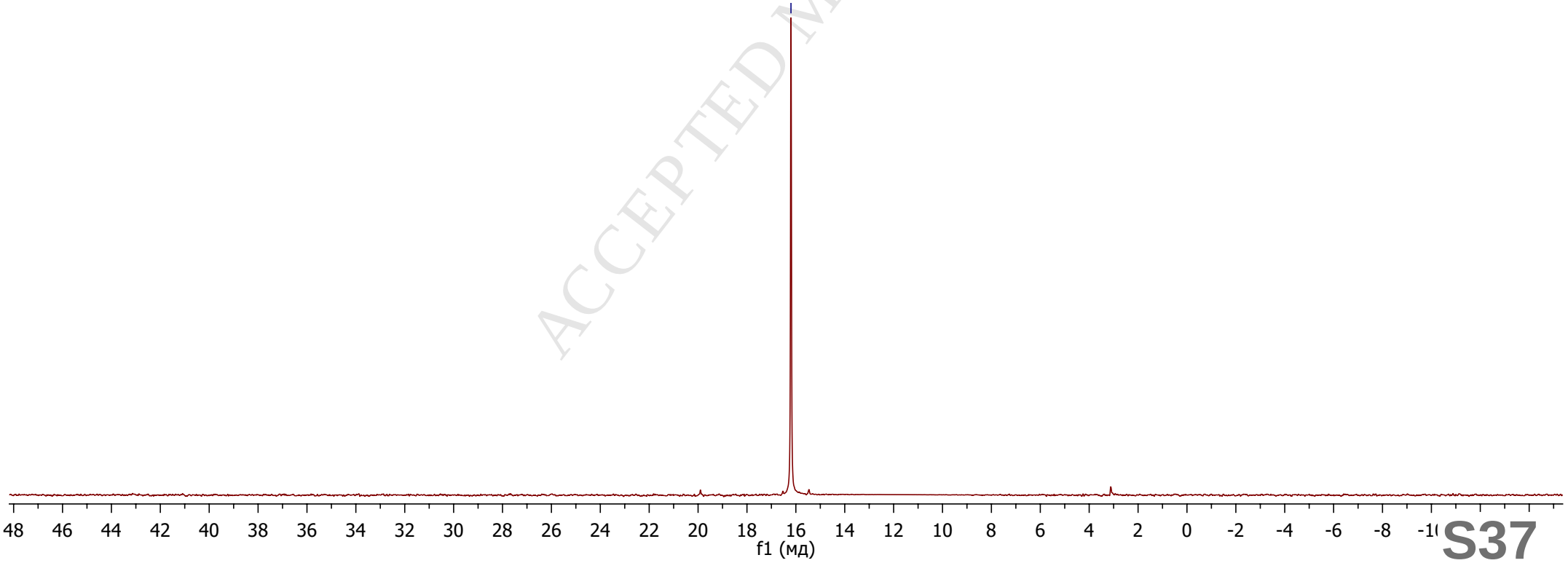

1H

BPH-4b

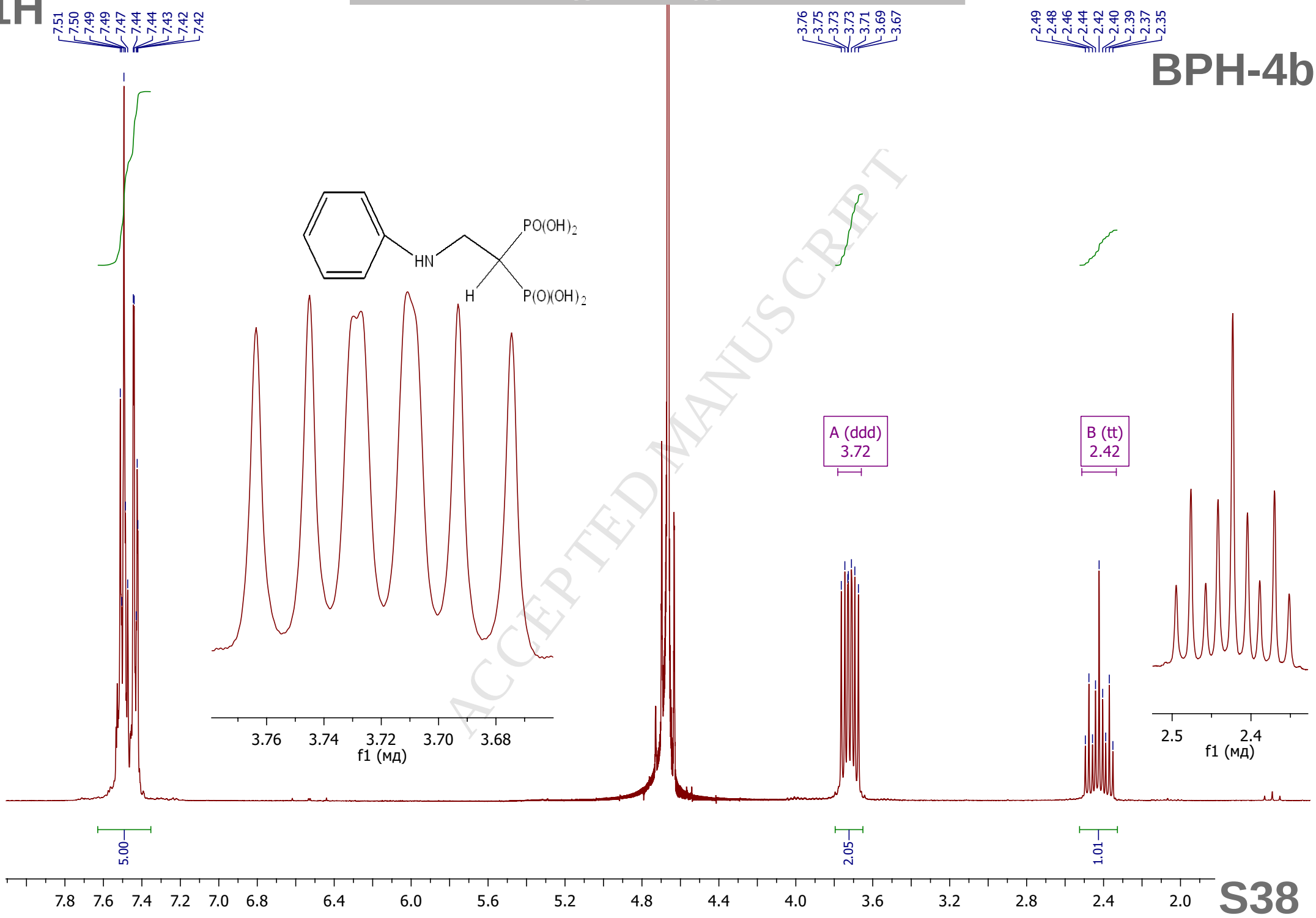

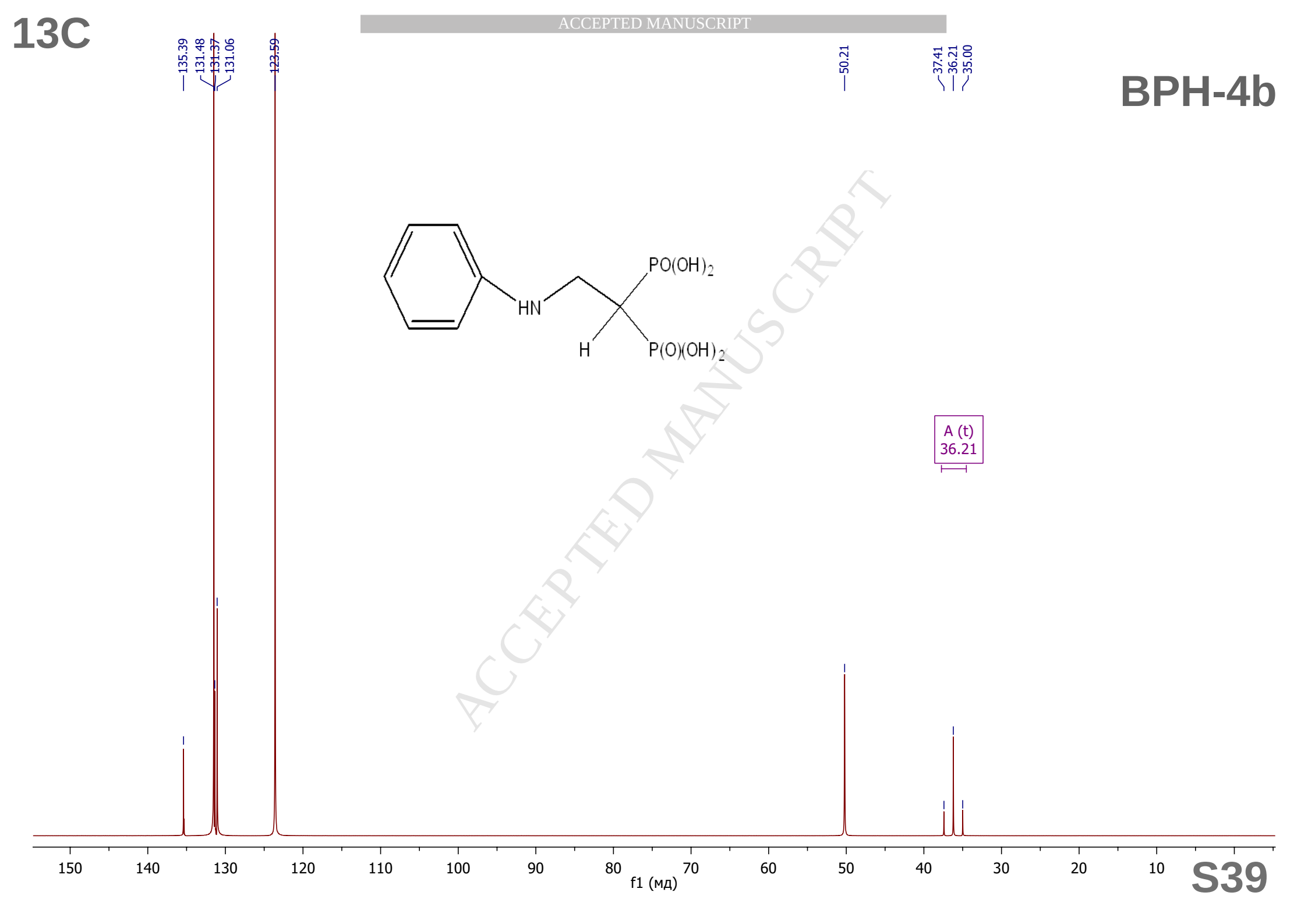

BPH-4b

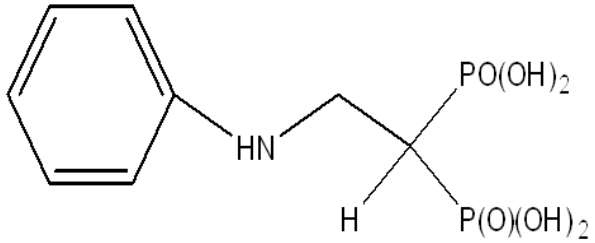

^{1}H NMR (400 MHz, D_2O) δ 7.52 (d, J = 8.7 Hz, 1H), 6.64 (d, J = 8.8 Hz, 1H), 3.45 (ddd, J = 26.7, 16.5, 9.9 Hz, 1H), 2.13 (tt, J = 20.5, 7.1 Hz, 1H).

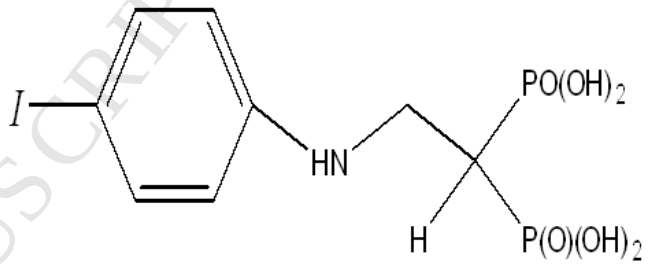

13C

BPH-4c

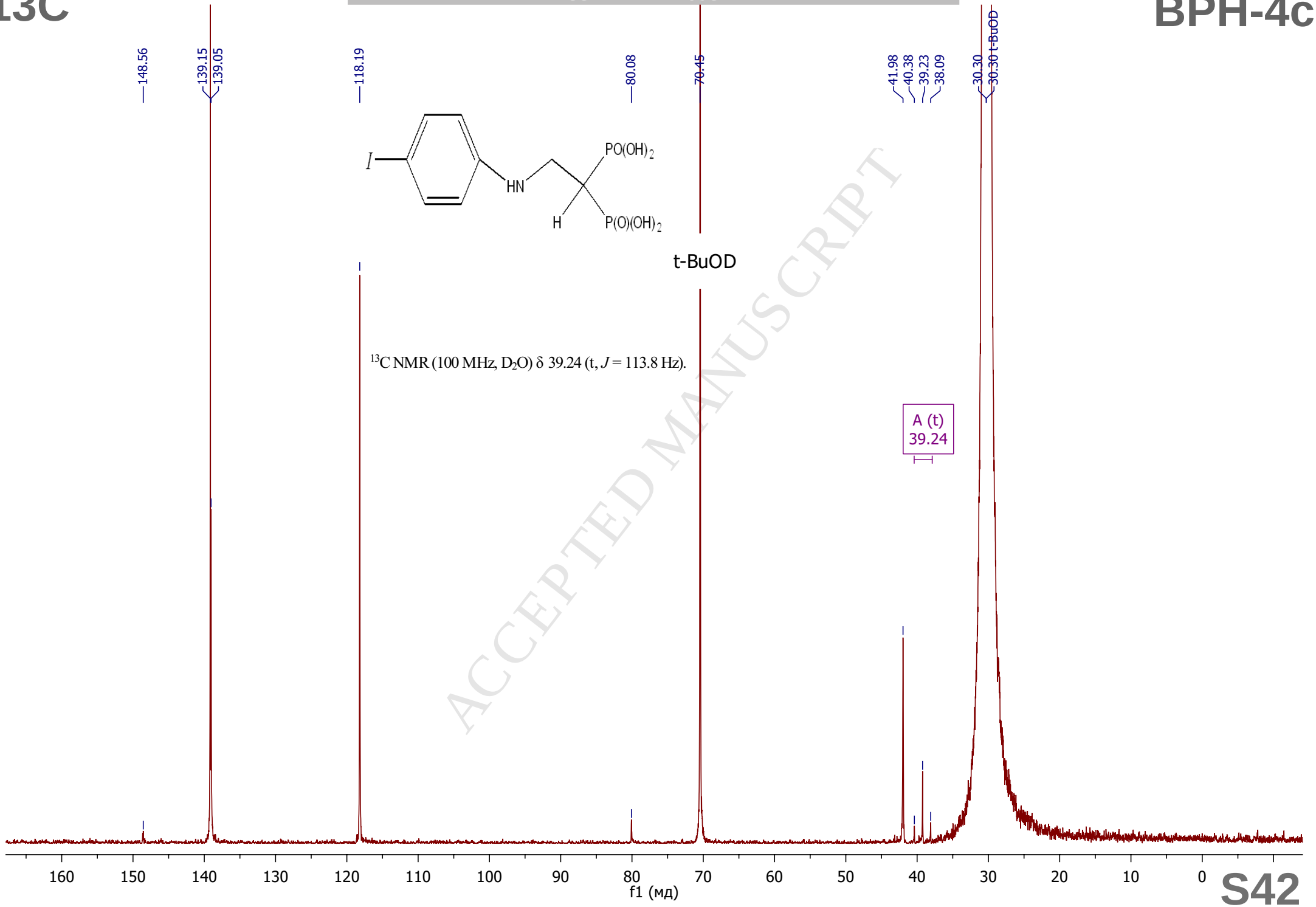

^{13}C NMR (100 MHz, D_2O) δ 39.24 (t, J = 113.8 Hz).

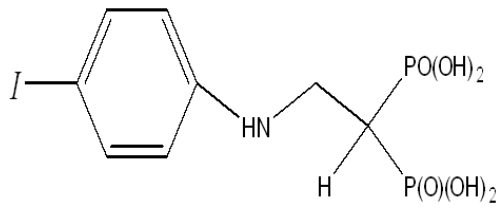

1H

BPH-5

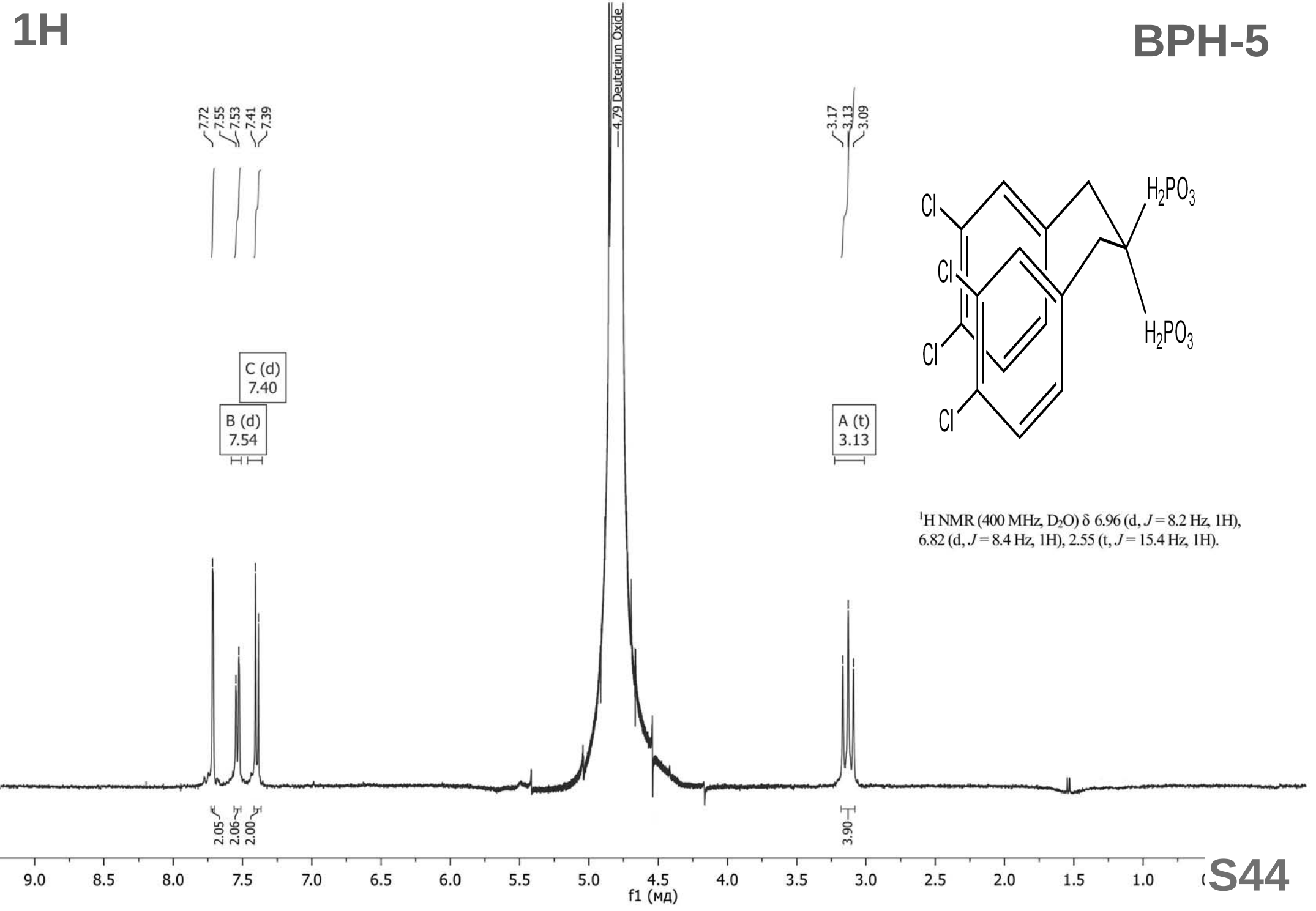

^{1}H NMR (400 MHz, D_2O) δ 6.96 (d, J = 8.2 Hz, 1H), 6.82 (d, J = 8.4 Hz, 1H), 2.55 (t, J = 15.4 Hz, 1H).

31P

BPH-5